

SANDIA REPORT

SAND2015-7963

Unlimited Release

Printed September 2015

Characterization of U.S. Wave Energy Converter (WEC) Test Sites: A Catalogue of Met-Ocean Data *2nd Edition*

Ann R. Dallman, Vincent S. Neary

Prepared by

Sandia National Laboratories

Albuquerque, New Mexico 87185 and Livermore, California 94550

Sandia National Laboratories is a multi-program laboratory managed and operated by Sandia Corporation, a wholly owned subsidiary of Lockheed Martin Corporation, for the U.S. Department of Energy's National Nuclear Security Administration under contract DE-AC04-94AL85000.

Approved for public release; further dissemination unlimited.



Sandia National Laboratories

Issued by Sandia National Laboratories, operated for the United States Department of Energy by Sandia Corporation.

NOTICE: This report was prepared as an account of work sponsored by an agency of the United States Government. Neither the United States Government, nor any agency thereof, nor any of their employees, nor any of their contractors, subcontractors, or their employees, make any warranty, express or implied, or assume any legal liability or responsibility for the accuracy, completeness, or usefulness of any information, apparatus, product, or process disclosed, or represent that its use would not infringe privately owned rights. Reference herein to any specific commercial product, process, or service by trade name, trademark, manufacturer, or otherwise, does not necessarily constitute or imply its endorsement, recommendation, or favoring by the United States Government, any agency thereof, or any of their contractors or subcontractors. The views and opinions expressed herein do not necessarily state or reflect those of the United States Government, any agency thereof, or any of their contractors.

Printed in the United States of America. This report has been reproduced directly from the best available copy.

Available to DOE and DOE contractors from
U.S. Department of Energy
Office of Scientific and Technical Information
P.O. Box 62
Oak Ridge, TN 37831

Telephone: (865) 576-8401
Facsimile: (865) 576-5728
E-Mail: reports@adonis.osti.gov
Online ordering: <http://www.osti.gov/bridge>

Available to the public from
U.S. Department of Commerce
National Technical Information Service
5285 Port Royal Rd
Springfield, VA 22161

Telephone: (800) 553-6847
Facsimile: (703) 605-6900
E-Mail: orders@ntis.fedworld.gov
Online ordering: <http://www.ntis.gov/help/ordermethods.asp?loc=7-4-0#online>



Characterization of U.S. Wave Energy Converter (WEC) Test Sites: A Catalogue of Met-Ocean Data

2nd Edition

Ann R. Dallman, Vincent S. Neary
Water Power Technologies
Sandia National Laboratories
P.O. Box 5800
Albuquerque, New Mexico 87185-MS1124

Abstract

This report presents met-ocean data and wave energy characteristics at eight U.S. wave energy converter (WEC) test and potential deployment sites. Its purpose is to enable the comparison of wave resource characteristics among sites as well as the selection of test sites that are most suitable for a developer's device and that best meet their testing needs and objectives. It also provides essential inputs for the design of WEC test devices and planning WEC tests, including the planning of deployment, and operations and maintenance. For each site, this report catalogues wave statistics recommended in the International Electrotechnical Commission Technical Specification (IEC 62600-101 TS) on Wave Energy Characterization, as well as the frequency of occurrence of weather windows and extreme sea states, and statistics on wind and ocean currents. It also provides useful information on test site infrastructure and services.

ACKNOWLEDGMENTS

This study was supported by the Department of Energy (DOE), Office of Energy Efficiency and Renewable Energy (EERE), Wind and Water Power Technologies Office (WWPTO). Sandia National Laboratories is a multi-program laboratory managed and operated by Sandia Corporation, a wholly owned subsidiary of Lockheed Martin Corporation, for the U.S. Department of Energy's National Nuclear Security Administration under contract DE-AC04-94AL85000.

The following people provided valuable input to this project:

- The bulk of the methodology for wave resource characterization used in this catalogue came from the now published International Electrotechnical Commission (IEC) Technical Specification (TS) on Wave Energy Resource Assessment and Characterization (IEC TS 62600-101 Ed. 1.0; also described in Folley et al. 2012). Much of this originated from work done at OSU (Lenée-Bluhm et al. 2011, Lenée-Bluhm 2010).
- Luis Vega (HINMREC, University of Hawaii (UH)), who provided information on the Wave Energy Test Site (WETS) and facilitated data analysis of the UH hindcast dataset for this catalogue. Kwok Fai Cheung and Ning Li at the University of Hawaii for providing the analysis of their hindcast dataset.
- Belinda Batten (OSU, NNMREC), who provided information on the North Energy Test Site (NETS) and South Energy Test Site (SETS) offshore of Newport, OR and feedback on the site descriptions.
- Tuba Özkan-Haller, Merrick Haller, and Gabriel García-Medina, (OSU), who provided helpful suggestions and feedback regarding the characterization methodology.
- Gabriel García-Medina (OSU), who provided the Oregon coast hindcast dataset (García-Medina et al. 2014) to Sandia National Laboratories for use in this catalogue.
- Pukha Lenée-Bluhm and Ken Rhinefrank, Columbia Power Technologies, for providing feedback on the methodology and data presented in the catalogue.
- Colin Sheppard, Humboldt State University, who provided information on the potential Humboldt Site and suggestions on the characterization methodology and presentation of data.
- Diana Bull, Water Power Technologies, Sandia National Laboratories, for providing information from previous wave resource assessment efforts near Humboldt Bay.
- Billy Edge and Lindsay Dubbs at the University of North Carolina Coastal Studies Institute for providing information on the Jennette's Pier Wave Energy Test Site and providing data from their hindcast for both the Jennette's Pier and the U.S. Army Corps of Engineers (USACE) Field Research Facility (FRF) sites.
- Michael Forte and Jeffrey Waters at the USACE FRF for providing information on the USACE FRF site.
- Kent Hathaway at the USACE FRF for providing historical measured data near the Jennette's Pier and USACE FRF sites.

- Jim Thomson at the Advanced Physics Laboratory at the University of Washington (APL-UW) for providing information on the Lake Washington site and providing buoy data from APL-UW measurement campaigns in the lake.
- Jonathan Berg, staff member at Sandia National Laboratories, who developed the first version of the MATLAB[®] script for the inverse form reliability method (IFORM) for generating environmental contours for extreme sea states.
- Aubrey Eckert-Gallup, staff member at Sandia National Laboratories, for estimating the extreme significant wave height for the selected sites that do not work well with IFORM.
- Jenessa Duncombe, summer student intern at Sandia National Laboratories, for gathering and organizing information for some of the site descriptions.
- Alex Campbell, summer student intern at Sandia National Laboratories, for processing some of the surface current and wind data.
- Christopher Simmons, student intern at Sandia National Laboratories, for processing surface current and wind data for the 2nd edition of the catalogue, and migrating the report to L^AT_EX.

CONTENTS

1. Introduction	29
1.1. Motivation	29
1.2. Wave Resource Characterization	29
1.3. Format of Report	31
2. Methodology	33
2.1. Overview	33
2.2. Data Presented	33
2.3. Data Sources	36
3. Pacific Marine Energy Test Center (PMEC): North Energy Test Site (NETS) . . .	39
3.1. Site Description	39
3.2. WEC Testing Infrastructure	41
3.2.1. Mooring Berths	41
3.2.2. Electrical Grid Connection	42
3.2.3. Facilitating Harbor	43
3.2.4. On-Shore Office Space	43
3.2.5. Service Vessel and Engineering Boatyard Access	43
3.2.6. Travel and Communication Infrastructure	43
3.2.7. Met-Ocean Monitoring Equipment	43
3.2.8. Environmental Monitoring	46
3.2.9. Permitting	46
3.3. Data used	46
3.4. Results	47
3.4.1. Sea States: Frequency of Occurrence and Contribution to Wave Energy	47
3.4.2. IEC TS Parameters	49
3.4.3. Cumulative Distributions	51
3.4.4. Weather Windows	52
3.4.5. Extreme Sea States	55
3.4.6. Representative Wave Spectrum	56
4. U.S. Navy Wave Energy Test Site (WETS)	59
4.1. Site Description	59
4.2. WEC Testing Infrastructure	62
4.2.1. Mooring Berths	62
4.2.2. Electrical Grid Connection	63
4.2.3. Facilitating Harbor	63
4.2.4. On-Shore Office Space	63
4.2.5. Service Vessel and Engineering Boatyard	64
4.2.6. Travel and Communication Infrastructure	64
4.2.7. Met-Ocean Monitoring Equipment	64

4.2.8.	Environmental Monitoring	67
4.2.9.	Permitting	67
4.3.	Data Used	67
4.4.	Results	68
4.4.1.	Sea States: Frequency of Occurrence and Contribution to Wave Energy	68
4.4.2.	IEC TS Parameters	71
4.4.3.	Cumulative Distributions	74
4.4.4.	Weather Windows	75
4.4.5.	Extreme Sea States	78
4.4.6.	Representative Wave Spectrum	79
5.	Jennette’s Pier Wave Energy Test Center	81
5.1.	Site Description	81
5.2.	WEC Testing Infrastructure	83
5.2.1.	Mooring Berths	83
5.2.2.	Electrical Grid Connection	83
5.2.3.	Facilitating Harbor	84
5.2.4.	On-Shore Office Space	84
5.2.5.	Service Vessel and Engineering Boatyard Access	84
5.2.6.	Travel and Communication Infrastructure	84
5.2.7.	Met-Ocean Monitoring Equipment	84
5.2.8.	Environmental Monitoring	86
5.2.9.	Permitting	87
5.3.	Data used	87
5.4.	Results	88
5.4.1.	Sea States: Frequency of Occurrence and Contribution to Wave Energy	89
5.4.2.	IEC TS Parameters	90
5.4.3.	Cumulative Distributions	92
5.4.4.	Weather Windows	93
5.4.5.	Extreme Sea States	96
5.4.6.	Representative Wave Spectrum	98
6.	U.S. Army Corps of Engineers (USACE) Field Research Facility (FRF)	101
6.1.	Site Description	101
6.2.	WEC Testing Infrastructure	103
6.2.1.	Mooring Berths	103
6.2.2.	Electrical Grid Connection	103
6.2.3.	Facilitating Harbor	104
6.2.4.	On-Shore Office Space	104
6.2.5.	Service Vessel and Engineering Boatyard Access	104
6.2.6.	Travel and Communication Infrastructure	104
6.2.7.	Met-Ocean Monitoring Equipment	104
6.2.8.	Environmental Monitoring	108
6.2.9.	Permitting	108
6.3.	Data used	108

6.4.	Results	109
6.4.1.	Sea States: Frequency of Occurrence and Contribution to Wave Energy	110
6.4.2.	IEC TS Parameters	111
6.4.3.	Cumulative Distributions	113
6.4.4.	Weather Windows	114
6.4.5.	Extreme Sea States	117
6.4.6.	Representative Wave Spectrum	119
7.	Pacific Marine Energy Test Center (PMEC): Lake Washington Test Site	121
7.1.	Site Description	121
7.2.	WEC Testing Infrastructure	123
7.2.1.	Mooring Berths	123
7.2.2.	Electrical Grid Connection	123
7.2.3.	Facilitating Harbor	124
7.2.4.	On-Shore Office Space	124
7.2.5.	Service Vessel and Engineering Boatyard Access	124
7.2.6.	Travel and Communication Infrastructure	124
7.2.7.	Met-Ocean Monitoring Equipment	124
7.2.8.	Environmental Monitoring	128
7.2.9.	Permitting	128
7.3.	Data used	128
7.4.	Results	128
7.4.1.	Sea States: Frequency of Occurrence and Contribution to Wave Energy	128
7.4.2.	IEC TS Parameters	130
7.4.3.	Cumulative Distributions	132
7.4.4.	Weather Windows	134
7.4.5.	Extreme Sea States	137
7.4.6.	Representative Wave Spectrum	139
8.	Pacific Marine Energy Test Center (PMEC): South Energy Test Site (SETS)	141
8.1.	Site Description	141
8.2.	WEC Testing Infrastructure	143
8.2.1.	Mooring Berths	143
8.2.2.	Electrical Grid Connection	143
8.2.3.	Facilitating Harbor	144
8.2.4.	On-Shore Office Space	144
8.2.5.	Service Vessel and Engineering Boatyard Access	144
8.2.6.	Travel and Communication Infrastructure	144
8.2.7.	Met-Ocean Monitoring Equipment	144
8.2.8.	Environmental Monitoring	147
8.2.9.	Permitting	147
8.3.	Data used	147
8.4.	Results	148
8.4.1.	Sea States: Frequency of Occurrence and Contribution to Wave Energy	148
8.4.2.	IEC TS Parameters	150

8.4.3.	Cumulative Distributions	152
8.4.4.	Weather Windows	153
8.4.5.	Extreme Sea States	156
8.4.6.	Representative Wave Spectrum	157
9.	CalWave Proposed Central Coast WEC Test Site at Vandenberg Air Force Base (VAFB)	159
9.1.	Site Description	159
9.2.	WEC Testing Infrastructure	161
9.2.1.	Mooring Berths	161
9.2.2.	Electrical Grid Connection	161
9.2.3.	Facilitating Harbor	162
9.2.4.	On-Shore Office Space	162
9.2.5.	Service Vessel and Engineering Boatyard Access	162
9.2.6.	Travel and Communication Infrastructure	162
9.2.7.	Met-Ocean Monitoring Equipment	163
9.2.8.	Environmental Monitoring	165
9.2.9.	Permitting	165
9.3.	Data used	166
9.4.	Results	167
9.4.1.	Sea States: Frequency of Occurrence and Contribution to Wave Energy	167
9.4.2.	IEC TS Parameters	169
9.4.3.	Cumulative Distributions	173
9.4.4.	Weather Windows	175
9.4.5.	Extreme Sea States	180
9.4.6.	Representative Wave Spectrum	182
10.	Humboldt Bay, California: Potential WEC Test Site	185
10.1.	Site Description	185
10.2.	WEC Testing Infrastructure	188
10.2.1.	Mooring Berths	188
10.2.2.	Electrical Grid Connection	188
10.2.3.	Facilitating Harbor	188
10.2.4.	On-Shore Office Space	188
10.2.5.	Service Vessel and Engineering Boatyard Access	188
10.2.6.	Travel and Communication Infrastructure	188
10.2.7.	Met-Ocean Monitoring Equipment	188
10.2.8.	Environmental Monitoring	192
10.2.9.	Permitting	192
10.3.	Data used	192
10.4.	Results	193
10.4.1.	Sea States: Frequency of Occurrence and Contribution to Wave Energy	194
10.4.2.	IEC TS Parameters	195
10.4.3.	Cumulative Distributions	197
10.4.4.	Weather Windows	198

10.4.5. Extreme Sea States	201
10.4.6. Representative Wave Spectrum	202
11. Summary and Conclusions	205
References	208
Appendix A. Pacific Marine Energy Center (PMEC): North Energy Test Site (NETS)	217
A.1. IEC TS Parameter Values	217
A.2. Wave Roses	218
A.3. Extreme Sea States	220
A.4. Wind Data	221
A.5. Ocean Surface Current Data	224
Appendix B. U.S. Navy Wave Energy Test Site (WETS)	227
B.1. IEC TS Parameter Values	227
B.2. Wave Roses	229
B.3. Extreme Sea States	231
B.4. Wind Data	232
B.5. Ocean Surface Current Data	235
Appendix C. Jennette’s Pier Wave Energy Test Center	239
C.1. IEC TS Parameter Values	239
C.2. Wave Roses	240
C.3. Extreme Sea States	241
C.4. Wind Data	243
C.5. Ocean Surface Current Data	246
Appendix D. U.S. Army Corps of Engineers (USACE) Field Research Facility (FRF)	249
D.1. IEC TS Parameter Values	249
D.2. Wave Roses	250
D.3. Extreme Sea States	251
D.4. Wind Data	253
D.5. Ocean Surface Current Data	256
Appendix E. Pacific Marine Energy Test Center (PMEC): Lake Washington Test Site	259
E.1. IEC TS Parameter Values	259
E.2. Wave Roses	260
E.3. Extreme Sea States	261
E.4. Wind Data	262
E.5. Ocean Surface Current Data	265
Appendix F. Pacific Marine Energy Test Center (PMEC): South Energy Test Site (SETS)	269
F.1. IEC TS Parameter Values	269
F.2. Wave Roses	270

F.3. Extreme Sea States	272
F.4. Wind Data	273
F.5. Ocean Surface Current Data	276
Appendix G. CalWave Proposed Central Coast WEC Test Site at Vandenberg Air Force Base (VAFB)	
G.1. IEC TS Parameter Values	279
G.2. Wave Roses	282
G.3. Extreme Sea States	284
G.4. Wind Data	286
G.5. Ocean Surface Current Data	289
Appendix H. Humboldt Bay, California: Potential WEC Test Site	
H.1. IEC TS Parameter Values	293
H.2. Wave Roses	294
H.3. Extreme Sea States	296
H.4. Wind Data	297
H.5. Ocean Surface Current Data	300

FIGURES

Figure 1	NETS is located in the coastal waters of Oregon near the City of Newport. The test site is 3-5 km off-shore in 45-55 m depth water. One National Data Buoy Center (NDBC) ocean buoy and one NDBC meteorological station are close to the site (see Table 1), as well as Oregon State University’s (OSU) test instrumentation buoy (see Section 3.2.7). The South Beach Marina, Port of Toledo Yaquina Boatyard, and OSU Hatfield Marine Science Center offer services valuable for WEC testing. The point of reference for the hindcast simulation is on the north edge of NETS. Image modified from Google Earth (Google Earth 2014).	40
Figure 2	Nautical chart of Yaquina Head and surrounding area shows the gradually sloping bathymetry around NETS. Soundings in fathoms (1 fathom = 1.8288 m). Image modified from nautical chart #18561 (Office of Coast Survey 2011).	41
Figure 3	The Ocean Sentinel acts as a grid emulator for WEC devices, as well as records electricity output and monitors surrounding environmental data. The WEC device is connected to the Ocean Sentinel via an umbilical cord.	42
Figure 4	(a) Moored buoy NDBC 46094 located 14 km southwest of the test site, (b) meteorological station NWPO3 on the coastline 8 km southeast of the test site (National Data Buoy Center 2014).	44

Figure 5	NETS location map showing CSFR wind and OSCAR surface current data points, and NDBC buoy locations (Google Earth 2015).	47
Figure 6	Joint probability distribution of sea states for NETS. The top figure is frequency of occurrence and the bottom figure is percentage of total energy, where total energy in an average year is 322,250 kWh/m.	49
Figure 7	The average, 5 th and 95 th percentiles of the six parameters at NETS.	50
Figure 8	The six parameters of interest over a one-year period, March 2007 – February 2008 at NETS.	51
Figure 9	Annual and seasonal cumulative distributions of the significant wave height (top) and energy period (bottom) at NETS.	52
Figure 10	Average cumulative occurrences of wave height thresholds (weather windows) for each season at NETS. Winter is defined as December – February, spring as March – May, summer as June – August, and fall as September – November.	53
Figure 11	Average cumulative occurrences of wave height thresholds (weather windows) for each season at NETS with an additional restriction of $U < 15$ mph.	54
Figure 12	Average cumulative occurrences of wave height thresholds (weather windows) for 6- and 12-hour durations with $U < 15$ mph and only during daylight hours (5am – 10pm LST) at NETS.	54
Figure 13	100-year contour for NDBC 46050 (1996–2014).	55
Figure 14	All hourly discrete spectra and the mean spectra measured at NDBC 46050 within the sea state listed above each plot. The JONSWAP and Bretschneider spectra are represented by red and black dotted lines, respectively.	57
Figure 15	WETS is located on the northeast shore of Oahu, Hawaii near the Marine Corps Base Hawaii (MCBH). The site is 1–2 km off-shore in 30-80 m depth water and has one operational berth and two berths under construction. One National Data Buoy Center ocean buoy and one National Data Buoy Center meteorological station are close to the site (see Table 2). The Heeia Kea Small Boat Harbor is located in Kaneohe Bay and a boatyard is accessible in Honolulu, HI. The hindcast simulation used two points of reference as shown. Image modified from Google Earth (2014).	60
Figure 16	Nautical Chart of Mokapu Peninsula and surrounding area shows the gradually sloping bathymetry at WETS. Soundings in fathoms (1 fathom = 1.8288 m). Image modified from nautical chart #19357 (Office of Coast Survey 2013).	61
Figure 17	WETS mooring configuration and bathymetry map showing underwater cables and the three mooring sites at 30 m, 60 m, and 80 m depth (De Visser and Vega 2014).	62
Figure 18	Sound & Sea Technology schematic of WETS 60 m and 80 m berths (De Visser and Vega 2014).	63
Figure 19	a) CDIP198 Waverider, b) CDIP098 Waverider (Coastal Data Information Program 2013).	65
Figure 20	Two wave buoys and one met station surround the test site. The data points for OSCAR and CSFR overlap at 21.5 N, 157.5 W (Google Earth 2014).	68

Figure 21	Joint probability distribution of sea states for the Kaneohe II berth (60 m depth). The top figure is frequency of occurrence and the bottom figure is percentage of total energy, where total energy in an average year is 114,450 kWh/m.	70
Figure 22	Joint probability distribution of sea states for the WETS berth (80 m depth). The top figure is frequency of occurrence and the bottom figure is percentage of total energy, where total energy in an average year is 125,850 kWh/m.	71
Figure 23	The average, 5 th and 95 th percentiles of the six parameters at Kaneohe II.	73
Figure 24	The average, 5 th and 95 th percentiles of the six parameters at WETS.	73
Figure 25	The six parameters of interest over a one-year period, March 2013 – February 2014 at NDBC 51207 co-located at the WETS 80 m berth.	74
Figure 26	Annual and seasonal cumulative distributions of the significant wave height (top) and energy period (bottom) at WETS.	75
Figure 27	Average cumulative occurrences of wave height thresholds (weather windows) for each season at WETS. Winter is defined as December – February, spring as March – May, summer as June – August, and fall as September – November.	76
Figure 28	Average cumulative occurrences of wave height thresholds (weather windows) for each season at WETS with an additional restriction of $U < 15$ mph.	77
Figure 29	Average cumulative occurrences of wave height thresholds (weather windows) for 6- and 12-hour durations with $U < 15$ mph and only during daylight hours (5am - 10pm LST) at WETS.	77
Figure 30	100-year contour for CDIP098/NDBC51202 (2001 – 2014).	78
Figure 31	All hourly discrete spectra and the mean spectra measured at CDIP198 / NDBC 51207 within the sea state listed above each plot. The JONSWAP and Bretschneider spectra are represented by red and black dotted lines, respectively.	80
Figure 32	Jennette’s Pier is located in the coastal waters of North Carolina in the town of Nags Head. The test site is 0.08 – 0.3 km off-shore in 6 – 11 m depth water. One National Data Buoy Center (NDBC) buoy is southeast of the site (see Table 3). The nearby UNC CSI is shown. Image modified from Google Earth (Google Earth 2015).	82
Figure 33	Nautical chart of Nags Head Island and the surrounding area shows the gradually sloping bathymetry off Jennette’s Pier. Soundings in feet (1 foot = 0.3048 m). Image modified from nautical chart #12204 (Office of Coast Survey 2015).	83
Figure 34	(a) CDIP 192 (NDBC 44095) located about 30 km southeast of the test site (Coastal Data Information Program 2013), (b) the AWAC being installed at the 11 m berth.	85
Figure 35	Jennette’s Pier & USACE FRF (see Chapter 6) location map showing CSFR wind and OSCAR surface current data points (Google Earth 2015).	88

Figure 36	Joint probability distribution of sea states for the Jennette’s Pier site. The top figure is frequency of occurrence and the bottom figure is percentage of total energy, where total energy in an average year is 53,300 kWh/m.	90
Figure 37	The average, 5 th and 95 th percentiles of the six parameters at the Jennette’s Pier site.	91
Figure 38	The six parameters of interest over a one-year period, March 2009 – February 2010 at the Jennette’s Pier site.	92
Figure 39	Annual and seasonal cumulative distributions of the significant wave height (top) and energy period (bottom) at the Jennette’s Pier site.	93
Figure 40	Average cumulative occurrences of wave height thresholds (weather windows) for each season at the Jennette’s Pier site. Winter is defined as December – February, spring as March – May, summer as June – August, and fall as September – November.	94
Figure 41	Average cumulative occurrences of wave height thresholds (weather windows) for each season at the Jennette’s Pier site with an additional restriction of $U < 15$ mph.	95
Figure 42	Average cumulative occurrences of wave height thresholds (weather windows) for 6- and 12-hour durations with $U < 15$ mph and only during daylight hours (5am – 10pm LST) at the Jennette’s Pier site.	95
Figure 43	The generalized extreme values distribution was fit to annual maximum of significant wave height from NDBC44056 to generate estimates of extreme values. The 95% confidence interval is shown as well.	97
Figure 44	The peak over thresholds method was used with a threshold value of the 99.5 th percentile of significant wave height from NDBC44056. The 95% confidence interval is shown as well.	98
Figure 45	All hourly discrete spectra and the mean spectra measured at AWAC05 within the sea state listed above each plot. The JONSWAP and Bretschneider spectra are represented by red and black dotted lines, respectively.	99
Figure 46	The USACE FRF is located in the coastal waters of North Carolina in the town of Duck. Three buoys, one AWAC, and one water level observation network close to the site are shown (see Table 4). Image modified from Google Earth (Google Earth 2015).	102
Figure 47	Nautical chart of Duck, NC and the surrounding area shows the gradually sloping bathymetry off Duck Pier. Soundings in feet (1 foot = 0.3048 m). Image modified from nautical chart #12204 (Office of Coast Survey 2015). End of Pier Coordinates: 36°11.02 N, 75°44.71 W.	103
Figure 48	(a) NDBC 44014 located 93 km northeast of the test site (National Data Buoy Center 2015), (b) CDIP 430 located 15 km northeast of the site (Field Research Facility, 2015).	105
Figure 49	Jennette’s Pier (see Chapter 5) & USACE FRF location map showing CSFR wind and OSCAR surface current data points (Google Earth 2015).	109
Figure 50	Joint probability distribution of sea states for the USACE FRF site. The top figure is frequency of occurrence and the bottom figure is percentage of total energy, where total energy in an average year is 28,815 kWh/m.	111

Figure 51	The average, 5 th and 95 th percentiles of the six parameters at the USACE FRF site.	112
Figure 52	The six parameters of interest over a one-year period, March 2008 – February 2009 at the USACE FRF site.	113
Figure 53	Annual and seasonal cumulative distributions of the significant wave height (top) and energy period (bottom) at the USACE FRF site.	114
Figure 54	Average cumulative occurrences of wave height thresholds (weather windows) for each season at the USACE FRF site. Winter is defined as December – February, spring as March – May, summer as June – August, and fall as September – November.	115
Figure 55	Average cumulative occurrences of wave height thresholds (weather windows) for each season at the USACE FRF site with an additional restriction of $U < 15$ mph.	116
Figure 56	Average cumulative occurrences of wave height thresholds (weather windows) for 6- and 12-hour durations with $U < 15$ mph and only during daylight hours (5am – 10pm LST) at the USACE FRF site.	116
Figure 57	The generalized extreme values distribution was fit to annual maximum of significant wave height from NDBC44056 to generate estimates of extreme values. The 95% confidence interval is shown as well.	118
Figure 58	The peak over thresholds method was used with a threshold value of the 99.5th percentile of significant wave height from NDBC44056. The 95% confidence interval is shown as well.	119
Figure 59	All hourly discrete spectra and the mean spectra measured at AWAC04 within the sea state listed above each plot. The JONSWAP and Bretschneider spectra are represented by red and black dotted lines, respectively.	120
Figure 60	PMEC Lake Washington is located in the northern portion of Lake Washington northeast of Seattle. The test site is approximately 1.2 km offshore in 56 m depth water. The fetch for predominant southerly winds in winter is about 5 km (from the Route 520 bridge). A Waverider buoy was deployed by APL-UW in three locations for short durations (see Table 5). Image modified from Google Earth (Google Earth 2015).	122
Figure 61	Nautical chart of part of Lake Washington shows the gradually sloping bathymetry around the test site. Soundings in feet (1 foot = 0.3048 m). Image modified from nautical chart #18447 (Office of Coast Survey 2012).	123
Figure 62	Waverider buoy deployed by the University of Washington located less than 1 km from the test site.	125
Figure 63	Joint probability distribution of sea states for Lake Washington. The top figure is frequency of occurrence and the bottom figure is percentage of total energy, where total energy in an average year is 177 kWh/m.	130
Figure 64	The average, 5 th and 95 th percentiles of the six parameters at the Lake Washington site.	131
Figure 65	The six parameters of interest over a one-year period, March 2013 – February 2014 at the Lake Washington site.	132
Figure 66	Annual and seasonal cumulative distributions of the significant wave height (top) and energy period (bottom) at the Lake Washington site.	133

Figure 67	Average cumulative occurrences of wave height thresholds (weather windows) for each season at the Lake Washington site. Winter is defined as December – February, spring as March – May, summer as June – August, and fall as September – November.	135
Figure 68	Average cumulative occurrences of wave height thresholds (weather windows) for each season at the Lake Washington site with an additional restriction of $U < 15$ mph.	136
Figure 69	Average cumulative occurrences of wave height thresholds (weather windows) for 6- and 12-hour durations with $U < 15$ mph and only during daylight hours (5am – 10pm LST) at the Lake Washington site.	136
Figure 70	The generalized extreme values distribution was fit to annual maximum of significant wave height from the hindcast dataset to generate estimates of extreme values. The 95% confidence interval is shown as well.	138
Figure 71	The peak over thresholds method was used with a threshold value of the 99.5th percentile of significant wave height from the hindcast dataset. The 95% confidence interval is shown as well.	139
Figure 72	All hourly discrete spectra and the mean spectra from the hindcast dataset within the sea state listed above each plot. The JONSWAP and Bretschneider spectra are represented by red and black dotted lines, respectively.	140
Figure 73	SETS is located in the coastal waters of Oregon near the City of Newport. The test site is approximately 11–13 km off-shore in 58–75 m depth water. One National Data Buoy Center (NDBC) ocean buoy and one NDBC meteorological station are close to the site (see Table 6). The South Beach Marina, Port of Toledo Yaquina Boatyard, and OSU Hatfield Marine Science Center offer services valuable for WEC testing. The point of reference for the hindcast simulation is in the center of SETS. Image modified from Google Earth (Google Earth 2015).	142
Figure 74	Nautical chart of Yaquina Head and surrounding area shows the gradually sloping bathymetry around SETS. Soundings in fathoms (1 fathom = 1.8288 m). Image modified from nautical chart #18561 (Office of Coast Survey 2011).	143
Figure 75	(a) Moored buoy NDBC 46094 located 9 km northwest of the test site, (b) meteorological station NWPO3 on the coastline 15 km northeast of the test site (National Data Buoy Center 2014).	145
Figure 76	SETS location map showing the CFSR wind and OSCAR surface current data points, and NDBC buoy locations (Google Earth 2015).	148
Figure 77	Joint probability distribution of sea states for SETS. The top figure is frequency of occurrence and the bottom figure is percentage of total energy, where total energy in an average year is 350,291 kWh/m.	150
Figure 78	The average, 5 th and 95 th percentiles of the six parameters at SETS.	151
Figure 79	The six parameters of interest over a one-year period, March 2007 – February 2008 at SETS.	152
Figure 80	Annual and seasonal cumulative distributions of the significant wave height (top) and energy period (bottom) at SETS.	153

Figure 81	Average cumulative occurrences of wave height thresholds (weather windows) for each season at SETS. Winter is defined as December – February, spring as March – May, summer as June – August, and fall as September – November.	154
Figure 82	Average cumulative occurrences of wave height thresholds (weather windows) for each season at SETS with an additional restriction of $U < 15$ mph.	155
Figure 83	Average cumulative occurrences of wave height thresholds (weather windows) for 6- and 12-hour durations with $U < 15$ mph and only during daylight hours (5am – 10pm LST) at SETS.	155
Figure 84	100-year contour for NDBC 46050 (1996–2014).	156
Figure 85	All hourly discrete spectra and the mean spectra measured at NDBC 46050 within the sea state listed above each plot. The JONSWAP and Bretschneider spectra are represented by red and black dotted lines, respectively.	158
Figure 86	Two of the potential Vandenberg test site areas, ‘South’, and ‘South by Southeast’ (SSE), are located on the coast of California near the city of Lompoc and Vandenberg Air Force Base. The South site is approximately 6-9 km off-shore in 71-109 m depth water (38.8-59.6 fathoms) and the South by Southeast site is approximately 6-11 km off-shore in 66-102 m depth water (36.1-55.8 fathoms). No berthing infrastructure exists at this time, however four potential berths at each site are signified by the blue circles. Two Coastal Data Information Program (CDIP) ocean buoys, and several National Weather Service (NWS) meteorological stations are close to the test site. The points of reference for the hindcast simulation data presented in this chapter are shown. Image modified from Google Earth (2015).	160
Figure 87	Nautical chart of the Vandenberg area offshore of Point Arguello and Point Conception shows the general bathymetry around the proposed test site. Soundings in fathoms (1 fathom = 1.8288 m). Image modified from nautical chart #18721 (Office of Coast Survey 2015).	161
Figure 88	(a) Waverider buoy CDIP071 / NDBC46218 located about 15 km southwest of test site (National Data Buoy Center 2015). (b) C-MAN Station PTGC1 located about 10 km north of test site (National Data Buoy Center 2015).	163
Figure 89	The catalogue test site locations in relation to OSCAR surface current and CSFR wind data points (Google Earth 2015).	166
Figure 90	Joint probability distribution of sea states for the South Vandenberg site. The top figure is frequency of occurrence and the bottom figure is percentage of total energy, where total energy in an average year is 352,980 kWh/m.	168
Figure 91	Joint probability distribution of sea states for the SSE Vandenberg site. The top figure is frequency of occurrence and the bottom figure is percentage of total energy, where total energy in an average year is 277,660 kWh/m. . .	169
Figure 92	The average, 5 th and 95 th percentiles of the six parameters at the South Vandenberg site.	171
Figure 93	The average, 5 th and 95 th percentiles of the six parameters at the SSE Vandenberg site.	171

Figure 94	The six parameters of interest over a one-year period, March 2003 – February 2004 at the South Vandenberg site.	172
Figure 95	The six parameters of interest over a one-year period, March 2003 – February 2004 at the SSE Vandenberg site.	173
Figure 96	Annual and seasonal cumulative distributions of the significant wave height (top) and energy period (bottom) at the South Vandenberg site. . . .	174
Figure 97	Annual and seasonal cumulative distributions of the significant wave height (top) and energy period (bottom) at the SSE Vandenberg site.	175
Figure 98	Average cumulative occurrences of wave height thresholds (weather windows) for each season at the South Vandenberg site. Winter is defined as December – February, spring as March – May, summer as June – August, and fall as September – November.	176
Figure 99	Average cumulative occurrences of wave height thresholds (weather windows) for each season at the South Vandenberg site with an additional restriction of $U < 15$ mph.	177
Figure 100	Average cumulative occurrences of wave height thresholds (weather windows) for 6- and 12-hour durations with $U < 15$ mph and only during daylight hours (5am – 10pm LST) at the South Vandenberg site.	177
Figure 101	Average cumulative occurrences of wave height thresholds (weather windows) for each season at the SSE Vandenberg site. Winter is defined as December – February, spring as March – May, summer as June – August, and fall as September – November.	178
Figure 102	Average cumulative occurrences of wave height thresholds (weather windows) for each season at the SSE Vandenberg site with an additional restriction of $U < 15$ mph.	179
Figure 103	Average cumulative occurrences of wave height thresholds (weather windows) for 6- and 12-hour durations with $U < 15$ mph and only during daylight hours (5am – 10pm LST) at the SSE Vandenberg site.	179
Figure 104	The generalized extreme values distribution was fit to annual maximum of significant wave height from NDBC46218 to generate estimates of extreme values. The 95% confidence interval is shown as well.	181
Figure 105	The peak over thresholds method was used with a threshold value of the 99.5th percentile of significant wave height from NDBC46218. The 95% confidence interval is shown as well.	182
Figure 106	All hourly discrete spectra and the mean spectra measured at CDIP071 / NDBC 46218 within the sea state listed above each plot. The JONSWAP and Bretschneider spectra are represented by red and black dotted lines, respectively.	183

Figure 107	The proposed Humboldt Site is located on the coast of California near the city of Eureka. The test site is 5-6 km off-shore in 45 m depth water (~25 fathoms). No berthing or ocean infrastructure exist at this time. A future grid connection could be established at the existing substation. Two National Data Buoy Center (NDBC) ocean buoys and two National Weather Service (NWS) meteorological stations are close to the test site. The Woodley Island Marina and the City of Eureka Public Marina are located in Humboldt Bay and boatyard access is available at the Fields Landing Boatyard. The point of reference for the hindcast simulation is the primary coordinate for the proposed test site. Image modified from Google Earth (2014).	186
Figure 108	Nautical chart of Humboldt Bay and surrounding area shows the general bathymetry around the proposed test site. Sounds in fathoms (1 fathom = 1.8288 m). For a detailed map of Humboldt Bay, see Nautical chart #18622 (Office of Coast Survey 2013). Image modified from nautical chart #18620 (Office of Coast Survey 2012).	187
Figure 109	(a) Discus buoy NDBC46022 located 30 km from site, (b) Waverider buoy CDIP128/NDBC46212 located 12 km south of test site (National Data Buoy Center 2014).	189
Figure 110	The catalogue test site location in relation to NDBC Buoys, OSCAR surface current data points, CSFR wind data points, and the nearest airport (Google Earth 2014).	193
Figure 111	Joint probability distribution of sea states for the Humboldt Site. The top figure is frequency of occurrence and the bottom figure is percentage of total energy, where total energy in an average year is 282,600 kWh/m. . . .	195
Figure 112	The average, 5th and 95th percentiles of the six parameters at the Humboldt site.	196
Figure 113	The six parameters of interest over a one-year period, March 2007 – February 2008 at the Humboldt site.	197
Figure 114	Annual and seasonal cumulative distributions of the significant wave height (top) and energy period (bottom) at the Humboldt site.	198
Figure 115	Average cumulative occurrences of wave height thresholds (weather windows) for each season at the Humboldt Site. Winter is defined as December - February, spring as March - May, summer as June - August, and fall as September - November.	200
Figure 116	Average cumulative occurrences of wave height thresholds (weather windows) for each season at the Humboldt Site with an additional restriction of $U < 15$ mph.	200
Figure 117	Average cumulative occurrences of wave height thresholds (weather windows) for 6- and 12-hour durations with $U < 15$ mph and only during daylight hours (5am – 10pm LST) at the Humboldt Site.	201
Figure 118	100-year contour for CDIP128 / NDBC 46212 (2004-2012).	202
Figure 119	All hourly discrete spectra and the mean spectra measured at CDIP128 / NDBC 46212 within the sea state listed above each plot. The JONSWAP and Bretschneider spectra are represented by red and black dotted lines, respectively.	204

Figure 120	Annual wave rose of omnidirectional wave power and direction of maximally resolved wave power. Values of J greater than 40 kW/m are included in the top bin as shown in the legend.	218
Figure 121	Annual wave rose of significant wave height and direction of maximally resolved wave power. Values of H_{m0} greater than 6 m are included in the top bin as shown in the legend.	219
Figure 122	Monthly wind velocity and direction obtained from CSFR data during the period 1/1/1979 to 12/31/2014 at 44.75 N, 124.5 W, located 30 km west/northwest of NETS (Figure 1).	221
Figure 123	(a) Annual and (b) seasonal wind roses of velocity and direction obtained from CSFR data during the period 1/1/1979 to 12/31/2014. Data taken at 44.75 N, 124.5 W, located approximately 30 km west/northwest of NETS (Figure 1).	222
Figure 124	Monthly ocean surface current velocity and direction obtained from OSCAR at 44.5 N, 125.5 W, located approximately 110 km southwest of NETS. Data period 1/1/1993 to 12/30/2014.	224
Figure 125	(a) Annual and (b) seasonal current roses of ocean surface current velocity and direction obtained from OSCAR at 44.5 N, 125.5 W. Data period 1/1/1993 to 12/30/2014.	225
Figure 126	Annual wave rose of omnidirectional wave power and direction of maximum directionally resolved wave power. Values of J greater than 40 kW/m are included in the top bin as shown in the legend. Figure produced by Ning Li (Li and Cheung 2014).	229
Figure 127	Annual wave rose of significant wave height and direction of maximum directionally resolved wave power. Values of H_{m0} greater than 6 m are included in the top bin as shown in the legend. Figure produced by Ning Li (Li and Cheung 2014).	230
Figure 128	Monthly wind velocity and direction obtained from CSFR data during the period 1/1/1979 to 12/31/2014 at 21.5 N, 157.5 W, located approximately 25 km east of WETS (Figure 20).	232
Figure 129	(a) Annual and (b) seasonal wind roses of velocity and direction obtained from CSFR data during the period 1/1/1979 to 12/31/2014. Data taken at 21.5 N, 157.5 W, located approximately 25 km east of WETS (Figure 20).	233
Figure 130	Monthly ocean surface current velocity and direction obtained from OSCAR at 21.5 N, 157.5 W, located approximately 25 km east of WETS. Data period 1/1/1993 to 12/30/2014.	235
Figure 131	(a) Annual and (b) seasonal current roses of ocean surface current velocity and direction obtained from OSCAR at 21.5 N, 157.5 W, located approximately 25 km east of WETS. Data period 1/1/1993 to 12/30/2014.	236
Figure 132	Annual wave rose of omnidirectional wave power and direction of maximally resolved wave power. Values of J greater than 40 kW/m are included in the top bin as shown in the legend.	240

Figure 133	Annual wave rose of significant wave height and direction of maximally resolved wave power. Values of H_{m0} greater than 6 m are included in the top bin as shown in the legend.	241
Figure 134	Monthly wind velocity and direction obtained from CSFR data during the period 1/1/1979 to 12/31/2014 at 36 N, 75.5 W, located approximately 12 km northeast of the the Jennette’s Pier site (Figure 35).	243
Figure 135	(a)Annual and (b) seasonal wind roses of velocity and direction obtained from CSFR data during the period 1/1/1979 to 12/31/14. Data taken at 36 N, 75.5 W, located approximately 12 km northeast of the the Jennette’s Pier site (Figure 35).	244
Figure 136	Monthly ocean surface current velocity and direction obtained from OSCAR at 36.5 N, 75.5 W, located approximately 60 km north/northeast of Jennette’s Pier. Data period 1/1/1993 to 12/31/2014.	246
Figure 137	(a) Annual and (b) seasonal current roses of velocity and direction obtained from OSCAR at 36.5 N, 75.5 W, located approximately 60 km north/northeast of Jennette’s Pier. Data period 1/1/1993 to 12/31/2014. . .	247
Figure 138	Annual wave rose of omnidirectional wave power and direction of maximally resolved wave power. Values of J greater than 40 kW/m are included in the top bin as shown in the legend.	250
Figure 139	Annual wave rose of significant wave height and direction of maximally resolved wave power. Values of H_{m0} greater than 4 m are included in the top bin as shown in the legend.	251
Figure 140	Monthly wind velocity and direction obtained from CSFR data during the period 1/1/1979 to 12/31/2014 at 36.25 N, 75.5 W.	253
Figure 141	(a) Annual and (b) seasonal wind roses of velocity and direction obtained from CSFR data during the period 1/1/1979 to 12/31/14 at 36.25 N, 75.5 W.	254
Figure 142	Monthly current velocity and direction obtained from CSFR data during the period 1/1/1993 to 12/31/2014 at 36.5 N, 75.5 W.	256
Figure 143	(a)Annual and (b) seasonal current roses of velocity and direction obtained from CSFR data during the period 1/1/1993 to 12/31/14 at 36.5 N, 75.5 W.	257
Figure 144	Annual wave rose of omnidirectional wave power and direction of maximally resolved wave power. Values of J greater than 0.5 kW/m are included in the top bin as shown in the legend.	260
Figure 145	Annual wave rose of significant wave height and direction of maximally resolved wave power. Values of H_{m0} greater than 1 m are included in the top bin as shown in the legend.	261
Figure 146	Monthly wind velocity and direction obtained from the SR 520 bridge weather station on Lake Washington during the period 1/1/2005 to 12/31/2014.	262
Figure 147	(a) Annual and (b) seasonal wind roses of velocity and direction obtained from the SR 520 bridge weather station during the period 1/1/2005 to 12/31/14.	263
Figure 148	Monthly current velocity and direction estimated using the SR 520 bridge wind data on Lake Washington during the period 1/1/2005 to 12/31/2014.	265

Figure 149 (a) Annual and (b) seasonal current roses of velocity and direction estimated using the SR 520 bridge wind data during the period 1/1/2005 to 12/31/14.	266
Figure 150 Annual wave rose of omnidirectional wave power and direction of maximally resolved wave power. Values of J greater than 40 kW/m are included in the top bin as shown in the legend.	270
Figure 151 Annual wave rose of significant wave height and direction of maximally resolved wave power. Values of H_{m0} greater than 6 m are included in the top bin as shown in the legend.	271
Figure 152 Monthly wind velocity and direction obtained from CSFR data during the period 1/1/1979 to 12/31/2014 at 44.5 N, 124.5 W, located 23 km west/southwest of SETS (Figure 76).	273
Figure 153 (a) Annual and (b) seasonal wind roses of velocity and direction obtained from CSFR data during the period 1/1/1979 to 12/31/2014.	274
Figure 154 Monthly ocean surface current velocity and direction obtained from OSCAR at 44.5 N, 125.5 W. Data period 1/1/1993 to 12/30/2014.	276
Figure 155 (a) Annual and (b) seasonal current roses of ocean surface current velocity and direction obtained from OSCAR at 44.5 N, 125.5 W. Data period 1/1/1993 to 12/30/2014.	277
Figure 156 Annual wave rose of omnidirectional wave power and direction of maximally resolved wave power at the South location. Values of J greater than 40 kW/m are included in the top bin as shown in the legend.	282
Figure 157 Annual wave rose of omnidirectional wave power and direction of maximally resolved wave power at the SSE location. Values of J greater than 40 kW/m are included in the top bin as shown in the legend.	283
Figure 158 Annual wave rose of significant wave height and direction of maximally resolved wave power at the South location. Values of H_{m0} greater than 6 m are included in the top bin as shown in the legend.	283
Figure 159 Annual wave rose of significant wave height and direction of maximally resolved wave power at the SSE location. Values of H_{m0} greater than 6 m are included in the top bin as shown in the legend.	284
Figure 160 Monthly wind velocity and direction obtained from CSFR data during the period 1/1/1979 to 12/31/2014 at 34.5 N, 121 W, located approximately 30 km west of the test site.	286
Figure 161 (a)Annual and (b) seasonal wind roses of velocity and direction obtained from CSFR data during the period 1/1/1979 to 12/31/14. Data taken at 34.5 N, 121 W, located approximately 30 km west of the test site.	287
Figure 162 Monthly current velocity and direction obtained from CSFR data during the period 1/1/1993 to 12/31/2014 at 34.5 N, 121.5 W.	289
Figure 163 (a)Annual and (b) seasonal current roses of velocity and direction obtained from CSFR data during the period 1/1/1993 to 12/31/14. Data taken at 34.5 N, 121.5 W.	290
Figure 164 Annual wave rose of omnidirectional wave power and direction of maximum directionally resolved wave power. Values of J greater than 40 kW/m are included in the top bin as shown in the legend.	294

Figure 165	Annual wave rose of significant wave height and direction of maximum directionally resolved wave power. Values of H_{m0} greater than 6 m are included in the top bin as shown in the legend.	295
Figure 166	Monthly wind velocity and direction obtained from CSFR data during the period 1/1/1979 to 12/31/2014 at 40.75 N, 124.5 W, located approximately 25 km southwest of the test site (Figure 110).	297
Figure 167	(a)Annual and (b) seasonal wind roses of velocity and direction obtained from CSFR data during the period 1/1/1979 to 12/31/14. Data taken at 40.75 N, 124.5 W, located approximately 25 km southwest of the test site.	298
Figure 168	Monthly ocean surface current velocity and direction obtained from OSCAR at 40.5 N, 125.5 W, located approximately 110 km southwest of the Humboldt Site. Data period 1/1/1993 to 12/30/2014.	300
Figure 169	(a)Annual and (b) seasonal current roses of ocean surface current velocity and direction obtained from OSCAR at 40.5 N, 125.5 W, located approximately 110 km southwest of the Humboldt Site. Data period 1/1/1993 to 12/30/2014.	301

TABLES

Table 1	Wave monitoring equipment in close proximity to NETS.	45
Table 2	Wave monitoring equipment in close proximity to WETS.	66
Table 3	Wave monitoring equipment in close proximity to Jennette’s Pier.	86
Table 4	Wave monitoring equipment in close proximity to the USACE FRF.	106
Table 5	Wave monitoring equipment in close proximity to PMEC Lake Washington.	126
Table 6	Wave monitoring equipment in close proximity to SETS. Note this is the same equipment provided for NETS in Table 1.	146
Table 7	Wave monitoring equipment in close proximity to the VAFB proposed test site.	164
Table 8	Wave monitoring equipment in close proximity to the Humboldt proposed test site.	190
Table 9	The average, 5 th and 95 th percentiles of the six parameters at NETS (see Figure 7).	217
Table 10	Selected values along the 100-year contour for NDBC46050 (see Figure 13).	220
Table 11	Monthly wind velocity and direction obtained from CSFR data during the period 1/1/1979 to 12/31/2014 at 44.75 N, 124.5 W, located approximately 30 km west/northwest of NETS.	223
Table 12	Monthly surface current velocity and direction obtained from OSCAR data during the period 1/1/1993 to 12/30/2014 at 44.5 N, 125.5 W.	226

Table 13	The average, 5 th and 95 th percentiles of the six parameters at Kaneohe II (see Figure 23).	227
Table 14	The average, 5 th and 95 th percentiles of the six parameters at WETS (see Figure 24).	228
Table 15	Selected values along the 100-year contour for CDIP098 (NDBC 51202) (see Figure 30).	231
Table 16	Monthly wind velocity and direction obtained from CSFR data during the period 1/1/1979 to 12/31/2014 at 21.5 N, 157.5 W, located approximately 25 km east of WETS.	234
Table 17	Monthly surface current velocity and direction obtained from OSCAR data during the period 1/1/1993 to 12/30/2014 at 21.5 N, 157.5 W, located approximately 25 km east of WETS.	237
Table 18	The average, 5 th and 95 th percentiles of the six parameters at Jennette's Pier (see Figure 37).	239
Table 19	Estimates of extreme significant wave height values using the generalized extreme value distribution (see Figure 43).	241
Table 20	Estimates of extreme significant wave height values using the peak over thresholds method (see Figure 44).	242
Table 21	Monthly wind velocity and direction obtained from CSFR data during the period 1/1/1979 to 12/31/2014 at 36 N, 75.5 W, located approximately 12 km northeast of Jennette's Pier.	245
Table 22	Monthly surface current velocity and direction obtained from OSCAR data during the period 1/1/1993 to 12/31/2014 at 36.5 N, 75.5 W, located approximately 60 km north/northeast of Jennette's Pier.	248
Table 23	The average, 5 th and 95 th percentiles of the six parameters at USACE FRF (see Figure 37).	249
Table 24	Estimates of extreme significant wave height values using the generalized extreme value distribution (see Figure 57).	251
Table 25	Estimates of extreme significant wave height values using the peak over thresholds method (see Figure 58).	252
Table 26	Monthly wind velocity and direction obtained from CSFR data during the period 1/1/1979 to 12/31/2014 at 36.25 N, 75.5 W, located approximately 23 km northeast of USACE FRF.	255
Table 27	Monthly surface current velocity and direction obtained from OSCAR data during the period 1/1/1993 to 12/30/2014 at 36.5 N, 75.5 W, located approximately 40 km northeast of the USACE FRF site.	258
Table 28	The average, 5 th and 95 th percentiles of the six parameters at Lake Washington (see Figure 64).	259
Table 29	Estimates of extreme significant wave height values using the generalized extreme value distribution (see Figure 70).	261
Table 30	Estimates of extreme significant wave height values using the peak over thresholds method (see Figure 71).	262
Table 31	Monthly wind velocity and direction obtained from the SR 520 bridge weather station on Lake Washington during the period 1/1/2005 to 12/31/2014.	264

Table 32	Monthly surface current velocity and direction estimates using the SR 520 bridge wind data during the period 1/1/2005 to 12/31/14.	267
Table 33	The average, 5 th and 95 th percentiles of the six parameters at SETS (see Figure 78).	269
Table 34	Selected values along the 100-year contour for NDBC46050 (see Figure 84).	272
Table 35	Monthly wind velocity and direction obtained from CSFR data during the period 1/1/1979 to 12/31/2014 at 44.5 N, 124.5 W, located approximately 23 km west/southwest of SETS.	275
Table 36	Monthly surface current velocity and direction obtained from OSCAR data during the period 1/1/1993 to 12/30/2014 at 44.5 N, 125.5 W.	278
Table 37	The average, 5 th and 95 th percentiles of the six parameters at the South Vandenberg site (see Figure 92).	280
Table 38	The average, 5 th and 95 th percentiles of the six parameters at the South by Southeast Vandenberg site (see Figure 93).	281
Table 39	Estimates of extreme significant wave height values using the generalized extreme value distribution (see Figure 104).	284
Table 40	Estimates of extreme significant wave height values using the peak over thresholds method (see Figure 105).	285
Table 41	Monthly wind velocity and direction obtained from CSFR data during the period 1/1/1979 to 12/31/2014 at 34.5 N, 121 W, located approximately 30 km west of the Vandenberg AFB site.	288
Table 42	Monthly surface current velocity and direction obtained from OSCAR data during the period 1/1/1993 to 12/31/2014 at 34.5 N, 121.5 W, located approximately 75 km from the site.	291
Table 43	The average, 5 th and 95 th percentiles of the six parameters at Humboldt (see Figure 112).	293
Table 44	Selected values along the 100-year contour for CDIP128 (NDBC 46212) (see Figure 118).	296
Table 45	Monthly wind velocity and direction obtained from CSFR data during the period 1/1/1979 to 12/31/2014 at 40.75 N, 124.5 W, located approximately 25 km southwest of the Humboldt site.	299
Table 46	Monthly surface current velocity and direction obtained from OSCAR data during the period 1/1/1993 to 12/30/2014 at 40.5 N, 125.5 W, located approximately 110 km from Humboldt test site.	302

NOMENCLATURE

ADCP	Acoustic Doppler Current Profiler
CDIP	Coastal Data Information Program
CFSR	Climate Forecast System Reanalysis
CFSv2	Climate Forecast System version 2
DOE	Department of Energy
EquiMar	Equitable Testing and Evaluation of Marine Energy Extraction Devices in terms of Performance, Cost and Environmental Impact
EMF	Electromagnetic Fields
ESA	Environmental Site Assessment
FERC	Federal Energy Regulatory Commission
HINMREC	Hawaii National Marine Renewable Energy Center
HNEI	Hawaii National Energy Institute
HSU	Humboldt State University
HWC	Humboldt WaveConnect
IEC	International Electrotechnical Commission
IFORM	Inverse First Order Reliability Method
MCBH	Marine Corps Base Hawaii
NETS	North Energy Test Site
NAVFAC	Naval Facilities Engineering Command
NDBC	National Data Buoy Center
NNMREC	Northwest National Marine Renewable Energy Center
NOAA	National Oceanic and Atmospheric Administration
OSCAR	Ocean Surface Current Analyses - Real time
OSU	Oregon State University
OWC	Oscillating Water Column
PG&E	Pacific Gas & Electric
PMEC	Pacific Marine Energy Center
PPLP	Pilot Project Licensing Process
SETS	South Energy Test Site
SNL	Sandia National Laboratories
TS	Technical Specification

UH	University of Hawaii
UNC CSI	University of North Carolina Coastal Studies Institute
USACE FRF	US Army Corps of Engineers Field Research Facility
VAFB	Vandenberg Air Force Base
WEC	Wave Energy Converter
WETS	Wave Energy Test Site
WET-NZ	Wave Energy Technology - New Zealand

1. INTRODUCTION

1.1. Motivation

The present study was motivated by the lack of a single information source that catalogues, with documented and consistent methodologies, met-ocean data and wave energy characteristics at U.S. wave energy converter (WEC) test sites and potential deployment sites. Such information allows WEC developers to compare wave resource characteristics among test sites as well as select test sites that are most suitable for their device and that best meet their testing needs and objectives. It also serves as an initial data set and framework to support a wave classification system, much like the wind classification system, which has become a standard for wind turbine design.

This catalogue includes wave statistics recommended in the International Electrotechnical Commission Technical Specification on Wave Energy Characterization (IEC TS 62600-101 Ed. 1.0; also described in Folley et al. 2012); but it also provides additional information on wave resource characteristics, including the frequency of occurrence of weather windows and extreme sea states, and statistics on wind and ocean currents. This additional information can assist developers in planning WEC tests, servicing their test devices, and assessing opportunities and risks at the test site.

1.2. Wave Resource Characterization

Wave energy resources are analyzed and presented in various ways throughout the literature. For example, efforts have included analyses of measured buoy data and/or hindcast simulation data; some consider full directional spectra while others only consider bulk parameters; extreme event analyses are often neglected or considered in separate studies. This ambiguity and difficulty in comparing assessments are some of the reasons that the IEC began the process of creating a technical specification (Folley et al. 2012). The IEC Technical Specification (TS) on Wave Energy Characterization is now completed and published (IEC TS 62600-101 Ed. 1.0).

Wave energy resource is defined in the IEC TS as “the amount of energy that is available for extraction from surface gravity waves,” (IEC TS 62600-101 Ed. 1.0). The TS includes guidelines for three classes of resource assessment. Class 1, or *reconnaissance*, is the lowest level and produces estimates with high uncertainty. This would be appropriate for large areas as the first assessment in a region. Class 2, or *feasibility*, produces estimates with greater certainty, and is appropriate for refining a reconnaissance assessment before a Class 3 assessment is done. Class 3, or *design*, produces an assessment with the least uncertainty and would be the final and most detailed assessment for small areas. This catalogue provides a Class 3 (*design*) assessment for the eight sites considered. For a detailed resource assessment at a particular site of interest, the energy characterization should be based on the analysis of directional wave spectra produced from a simulated hindcast. Measurements (e.g., from

buoys) can be useful for boundary conditions, and independent measured data should be used to validate the hindcast model.

In a related effort to the IEC TS, EquiMar (Equitable Testing and Evaluation of Marine Energy Extraction Devices in terms of Performance, Cost and Environmental Impact), published wave resource assessment guidance, Deliverable 2.7 (Davey et al. 2010), available at <http://www.equimar.org/equimar-project-deliverables.html>. According to this protocol, an assessment should provide an estimate of the available energy and the operating and survival characteristics of a site, which can be achieved by using a combination of in-situ measurements and numerical modelling. Similarly to the IEC TS, three stages of resource assessment are addressed, and the one closest to the IEC TS ‘design’ would be the EquiMar ‘Project Development,’ which should provide “detailed information on a deployment site including information on spectra and extremes,” (Davey et al. 2010). The period of record of data considered should be 10 years, and many cases would use numerical modeling. The EquiMar resource assessment is in general consistent with the IEC TS methodology adopted in this catalogue. The EquiMar project issued a brief catalogue, where several test sites were characterized with the best data available (O’Connor and Holmes 2011).

The IEC TS, and recent papers regarding the U.S. Pacific Northwest coast (Lenée-Bluhm et al. 2011, García-Medina et al. 2014), recommend six parameters to characterize the wave resource at a test site. In addition, they advocate calculating these parameters from simulated hindcast spectral wave data. These six parameters are omnidirectional wave power, significant wave height, energy period, spectral width, direction of maximum directionally resolved wave power, and directionality coefficient. Equations for calculating these statistics are provided in the Methodology section.

The IEC TS recommends that seasonal variation of wave statistics be considered, and monthly plots of the six parameters, along with seasonal cumulative distributions, should be provided. It also recommends that wave roses and time histories of the six parameters for one representative year be included. Wave roses provide a direct and intuitive means to visualize wave directions for corresponding wave bulk properties, typically omnidirectional wave power and significant wave height.

Although extreme sea states are not addressed in the IEC TS, they provide critical information needed to assess the risks of deploying a WEC at the test site and to design a WEC to survive wave loads associated with extreme sea states of a given return period. For this reason, the 100-year environmental contours are provided, as explained in Section 2.2. Although 100-year recurrence intervals (return periods) are common for marine structures, lower return periods can be used, if acceptable for survivability, when the design service life is less than 100 years (DNV 2005).

Additional wave statistics and met-ocean data, not specified in the IEC TS, but provided in this report, include weather windows as well as wind and ocean current statistics. This information is also valuable to developers for the purpose of assessing risks at the site and planning for testing and servicing of the WEC test device.

1.3. Format of Report

Three high energy wave sites were included in the First Edition of the catalogue, which was released in 2014: (1) the Pacific Marine Energy Center (PMEC) North Energy Test Site (NETS) offshore of Newport, Oregon; (2) Kaneohe Bay Naval Wave Energy Test Site (WETS) offshore of Oahu, HI; and (3) a potential test site offshore of Humboldt Bay (Eureka, CA). Five additional sites are now included in this edition of the catalogue: (4) the Jennette’s Pier Wave Energy Converter Test Site in North Carolina; (5) the US Army Corps of Engineers (USACE) Field Research Facility (FRF) offshore of Duck, North Carolina; (6) the PMEC Lake Washington test site; (7) the proposed PMEC South Energy Test Site (SETS) offshore of Newport, Oregon; and (8) the proposed CalWave Central Coast WEC Test Site at Vandenberg Air Force Base (VAFB).

Chapter 2 describes the methodology, including the data presented, analysis procedures, and data sources. Next is a chapter for each site (Chapters 3 - 10) that include descriptions of the site and testing infrastructure, and a discussion of the results of the met-ocean data. The established test sites are presented first, and potential test sites follow. A summary of the study and conclusions are presented in the final chapter (Chapter 11). Additional data is provided in plots and tables in the appendices.

2. METHODOLOGY

2.1. Overview

For this study, the third-generation phase-averaged spectral model SWAN (Simulating Waves Nearshore) was used to generate all wave climate hindcasts, from which wave statistics are calculated. For NETS and SETS, hindcast data was generated by researchers at the Northwest National Marine Renewable Energy Center (NNMREC) (García-Medina et al. 2014). The dataset for WETS was generated by the Hawaii National Marine Renewable Energy Center (HINMREC) (Li & Cheung 2014, Li et al. 2015). The datasets for the Jennette’s Pier and USACE FRF sites was generated by the University of North Carolina Coastal Studies Institute (UNC CSI). The dataset for Lake Washington was generated by Coast & Harbor (Coast and Harbor Engineering 2015). The CalWave VAFB data was generated by Humboldt State (see Appendix in Williams et al. 2015). Finally, for the Humboldt site, the dataset was generated by Sandia National Laboratories (Dallman et al. 2014). All hindcast simulations were validated by comparing predicted wave statistics against buoy observations prior to processing data and plots presented in this catalogue. HINMREC analyzed hindcast wave data for WETS, while Sandia National Laboratories (SNL) analyzed hindcast wave data for the rest of the sites.

2.2. Data Presented

The six parameters recommended by Lenee-Bluhm et al. (2011) and specified in the TS are defined below as in Lenee-Bluhm et al. (2011) and García-Medina et al. (2014). Equations for these parameters are repeated below for completeness.

The omnidirectional wave power, J , which indicates the resource available, is the sum of the contributions to energy flux from each of the components of the wave spectrum,

$$J = \sum_i \rho g c_{g,i} S_i \Delta f_i \quad (1)$$

where ρ is the density of sea water, g is the acceleration due to gravity, $c_{g,i}$ is the group velocity, S_i is the variance density, and Δf_i is the frequency bin width at each discrete frequency index i . Significant wave height, H_{m0} , estimated from spectra, is commonly used to describe the sea state and is defined as

$$H_{m0} = 4\sqrt{m_0} \quad (2)$$

where m_0 is the zeroth moment of the variance spectrum. The moments of variance spectrum are

$$m_n = \sum_i f_i^n S_i \Delta f_i. \quad (3)$$

The energy period, T_e , is also widely used to describe the sea state and is more robust than the peak period (due to a high sensitivity to spectral shape). The energy period is calculated

as

$$T_e = \frac{m_{-1}}{m_0}. \quad (4)$$

The spectral width,

$$\epsilon_0 = \sqrt{\frac{m_0 m_{-2}}{m_{-1}^2} - 1}, \quad (5)$$

characterizes the spreading of energy along the wave spectrum. The directionally resolved wave power is the sum of the wave power at each direction θ

$$J_\theta = \sum_{i,j} J_{ij} \Delta f_i \Delta \theta_j \cos(\theta - \theta_j) \delta \quad (6)$$

$$\begin{cases} \delta = 1, & \cos(\theta - \theta_j) \geq 0 \\ \delta = 0, & \cos(\theta - \theta_j) < 0 \end{cases}$$

where J is the directionally resolved wave power in direction θ . The maximum time averaged wave power propagating in a single direction, J_{θ_J} , is the maximum value of J_θ . The corresponding direction, θ_J , is the direction of maximum directionally resolved wave power and describes the characteristic direction of the sea state. The directionality coefficient, d_θ , is the ratio of maximum directionally resolved wave power to the omnidirectional wave power,

$$d_\theta = \frac{J_{\theta_J}}{J} \quad (7)$$

which is a characteristic measure of directional spreading of wave power (i.e., larger values approaching unity signify narrow directional spread). It is also recommended in the IEC TS that annual and seasonal values be reported.

The average monthly values of the above parameters, along with 5th and 95th percentiles, are presented to capture their variation over a typical year. This information is useful for planning deployments and tests. Optimal deployment windows, for example, are generally in summer months when sea states are less energetic than winter months. For similar reasons, testing of a scaled model WEC is generally more suitable in summer months.

Joint probability distribution (JPD) plots are presented to provide an overall depiction of the wave climate at each site and help inform the design of the WEC test device. These plots also include the mean, 5th and 95th percentiles of wave steepness, defined in this study as the ratio of the significant wave height to length, H_{m0}/γ , where the wavelength is calculated using the Newton-Raphson method to solve the dispersion relation (Holthuijsen 2007) using T_e . Steepness is important because it is related to wave breaking, and it affects wave forces on marine structures such as a WEC (Bitner-Gregersen 2001).

JPD plots, also known as bi-variate scatter plots (Cahill and Lewis 2013), can be used to present the frequency of occurrence of sea states (H_{m0} , T_e pairings) at a site, or the percentage contribution of each sea state to the total annual energy or power density. Wave characterization studies have shown (e.g., Cahill and Lewis 2011, Cahill and Lewis 2013, Lenee-Bluhm et al. 2011) that the sea states that occur most often do not necessarily correspond to those contributing the most to annual energy.

Cumulative distributions of H_{m0} and T_e are shown to describe the percentage of time these parameters are equal to or less than a threshold value. In order to account for duration, weather windows for wave heights equal to or less than threshold values are calculated for multiples of 6-hour periods. Weather windows quantify the number of opportunities in a given season or year to access the site for installation of a test device, or for operations and maintenance, based on their specific device, service vessels, and diving operation constraints.

Following suggestions from the IEC TS, wave roses are generated to visualize the spread and predominant directions of omnidirectional wave power and significant wave height. Rose plots for wind and ocean currents are also generated to examine the spread and predominant direction of wind and ocean currents. From these rose plots, one can also determine the percentage of time that a given statistical parameter (e.g., omnidirectional wave power) is equal or less than a given value at a specified direction sector. The radial thickness of a given bin represents the percentage of the time that the given omnidirectional wave power and direction occurs. Wave, wind, and current directions are defined as degrees clockwise from North. When directions are concentrated around North (0°), plots show positive directions (clockwise from North) and negative directions which are counter-clockwise from North. For example, -45° is equivalent to 315° .

Estimates of extreme sea states (H_{m0} , T_e pairings) are determined from 100-year environmental contours calculated using a modified version of the inverse first order reliability method (IFORM). The IFORM, as described by Winterstein et al. (1993), is standard design practice for generating environmental contours used for estimating extreme sea states of a given recurrence interval or return period (DNV 2014). It provides developers, not only with an estimate of the largest significant wave height, but also extreme sea states at other significant wave heights with energy periods that could compromise the survival of a marine structure or service vessel. The modified IFORM used in this study (Eckert-Gallup et al. 2014, Eckert-Gallup et al. 2016) improves the original fitting method by implementing principal components analysis. MATLAB[®] scripts to estimate contours using this modified IFORM were created by Sandia National Laboratories and are available on the Water Power website. As currently implemented, neither the IFORM nor the modified IFORM work well for datasets whose variables (H_{m0} and T_e) are bimodally distributed. Such distributions lead to complex dependencies between the variables that cannot be captured by the expression of joint probability used in either method, leading to erroneous representations of extreme sea state contours. This bimodality can be found in the buoy data representing the North Carolina and CalWave Vandenberg sites. For this reason, only the 100 year significant wave height, estimated through the application of extreme value theory, is presented at these sites. This was estimated using two extreme value theory methods for completeness: the generalized extreme value distribution (GEV) and peak over threshold (POT) method. Further details are provided in the chapters for these sites. Lake WA will also be an exception using extreme value theory because the distribution is so narrow due to the waves being short fetched wind waves (see Section 7.4.5).

Estimates of applied wave loads and power response under a diverse range of sea states is required for designing and siting a WEC. Since running simulations for a WEC response to all

frequency spectra occurring at a site would take an unfeasibly long amount of time, it is beneficial to synthesize a fixed number of spectra which can be used to represent each expected sea state (e.g., Lenee-Bluhm 2010). Therefore, representative spectra for the most common sea states at a site (found in the JPD) were calculated by averaging all measured spectra within each sea state. Standard spectra (Bretschneider and JONSWAP) were included for comparison.

The Bretschneider spectrum, which is meant for developing seas, was computed according to the unified form described in Chakrabarti (1987),

$$S(\omega) = \frac{A}{4} H_{m0}^2 \omega_s^4 \omega^{-5} \exp\left(-A \left(\frac{\omega}{\omega_s}\right)^{-4}\right), \quad (8)$$

where $A = 0.675$ is a nondimensional constant and $\omega_s = T_p/1.167$ is the significant frequency. The JONSWAP spectrum (Hasselmann et al. 1973), is an extension of the Pierson-Moskowitz spectrum (for fully developed wind seas) to include fetch-limited wind seas, and therefore describes developing seas. It was computed according the DNV Recommended Practices on Environmental Conditions and Environmental Loads (DNV-RP-C205 2014),

$$S(\omega) = A_\gamma \frac{5}{16} H_{m0}^2 \omega_p^4 \omega^{-5} \exp\left(-\frac{5}{4} \left(\frac{\omega}{\omega_s}\right)^{-4}\right) \gamma^{\exp\left(-0.5 \left(\frac{\omega - \omega_p}{\sigma \omega_p}\right)^2\right)}, \quad (9)$$

where $\omega_p = 2\pi/T_p$ is the angular spectral peak frequency, $A_\gamma = 1 - 0.287 \ln(\gamma)$ is a normalizing factor, $\gamma = 3.3$ is a non-dimensional shape parameter, and σ is a spectral width parameter where $\sigma = 0.07$ for $\omega \leq \omega_p$ and $\sigma = 0.09$ for $\omega \geq \omega_p$. If the wind speed and fetch were known, the JONSWAP spectrum could be calculated according to the equation in Hasselmann et al. (1973). Use of this equation, however, does not ensure the spectrally estimated H_{m0} would match the input value. Although a better fit could be achieved if a least squares fit was applied to the mean of the measured spectrum, it is assumed that the actual spectral shape would not be known *a priori* and a standard spectrum would be fit to a sea state (H_{m0} , T_e or T_p). Therefore, this comparison shows how well an assumed standard spectrum fits an actual measured spectrum without knowing the shape *a priori*.

As well as wave statistics, monthly averages of wind speed and direction, along with seasonal and annual wind roses are provided for each site. Monthly averages of ocean surface current speed and direction, along with seasonal and annual current roses are provided for each site.

2.3. Data Sources

The majority of the wave climate statistics (e.g., the six parameters of interest described above) were calculated from validated hindcast model simulations, as recommended in the IEC TS. These hindcast datasets are described in the Data Used section for each site.

In general, these phase averaged wave models do not simulate large waves well (for example the hindcast by García-Medina et al. 2014, represents significant wave height only up

to $H_{m0} \approx 8m$), unless specialized input data and versions of models are used for specific storms (e.g., the National Weather Services National Hurricane Center specialized models). Therefore the hindcast models utilized in this catalogue may not be reliable data sources for estimations of extreme events. The location of a buoy at each site does not necessarily coincide with the actual test site, but it is the most reliable data source for this calculation, and is used herein. In addition, results in Feld & Mork (2004) indicate that hindcast model spectra are less peaked than measured buoy data, and therefore representative spectra are also calculated from buoy data. The location and POR of buoys used will be described in each chapter.

Wind data for each site was obtained from 0.5 degree spatial resolution and 6-hour temporal resolution datasets available at the National Centers for Environmental Predictions (NCEP) Climate Forecast System Reanalysis (CFSR) (covering 1979-2010) and CFSv2 (covering 2011-present) (Saha et al. 2010, Saha et al. 2014). Data was selected at a single point or multiple points closest to the site. When multiple points were selected a simple arithmetic average of the data reported at each time step was computed. The wind data available from buoys or onshore meteorological stations greatly varies between sites, so using CFSR allows for a consistent data source between sites. In addition, CFSR data generally has better spatial coverage than buoy data, as well as longer periods of record (POR). The exception to this is the Lake Washington site because CFSR data is not available directly over the lake, and data over nearby land is not a reliable estimate of the local winds. Therefore a met tower on a bridge over the lake is used for that site.

Surface currents near the test sites were obtained from Ocean Surface Current Analyses Real time (OSCAR), part of the National Oceanic and Atmospheric Administration (NOAA). OSCAR calculates near real-time global sea surface currents from NASA satellite data and reports the data publically on their website. Sea surface currents are calculated from (1) sea surface height derived from Satellite altimeter and (2) ocean near-surface wind speed and direction from satellite scatterometers. The result is a global-scale sea surface current speed and direction dataset with a spatial resolution of 1 degree and a temporal resolution of 5 days.

OSCAR current data has been shown to be accurate for time-mean measurements by Johnson et al.(2007). Compared to moored current meters, drifters and shipboard current profilers, OSCAR mean sea surface currents closely match observed data at all latitudes and longitudes. High frequency (HF) radar has a higher resolution and is often a preferred data source for real-time applications and short term analyses, but is unavailable at the Hawaii site and has a much shorter period of record compared to OSCAR. As more systems are setup along the U.S. coast and the POR increases, HF radar will likely become a viable data source for long term characterization. For the purpose of this catalogue, OSCAR data was used because it provides data at each site to maintain consistency, has periods of record of at least 10 years at each site, and has been shown to be accurate for mean current speed and direction. Again, the exception to this is the Lake Washington site, where OSCAR data is unavailable. An estimate of surface currents based on the wind data is provided, and is explained in that chapter.

3. PACIFIC MARINE ENERGY TEST CENTER (PMEC): NORTH ENERGY TEST SITE (NETS)

3.1. Site Description

The Pacific Marine Energy Center (PMEC) is the name of the Northwest National Marine Renewable Energy Centers (NNMREC) marine energy converter testing facilities located in the Pacific Northwest region. NNMREC is a Department of Energy funded entity designed to facilitate development of marine renewable energy technology. Ultimately PMEC will facilitate testing a broad range of technologies being produced by the marine energy industry (NNMREC 2014). The North Energy Test Site (NETS) is an off-grid WEC test site that became operational in the summer of 2012. As shown in Figure 1, it encompasses an area of 1-square nautical mile (roughly 3 square kilometers) within state waters at 44.6899 N, 124.1346 W.

NETS is located near the City of Newport, Oregon and Yaquina Bay. At the test site, the water depth is approximately 45-55 m (25-30 fathoms), the bathymetry is gently sloping, and the sea bed consists of soft sand. Figure 2 shows the bathymetry surrounding promontory Yaquina Head and the test site. The wave climate at the test site varies seasonally, with calmer seas in the summer compared to more energetic seas in the winter. The wave environment at NETS is characterized by an annual average power flux of about 37 kW/m, including a number of events with significant wave heights exceeding 7 m each winter.

NNMREC offers a wide range of technical and testing infrastructure support services for WEC developers, including access to a fully instrumented test buoy and grid connection emulator at NETS. NETS has full scale wave energy resources, and can accommodate devices up to 100 kW connected to the mobile ocean test berth, the Ocean Sentinel, and larger devices if no grid emulation or connection is required.

NNMREC is currently designing a utility-scale, grid-accessible test site, the South Energy Test Site (SETS), which is planned to be operational in 2017.

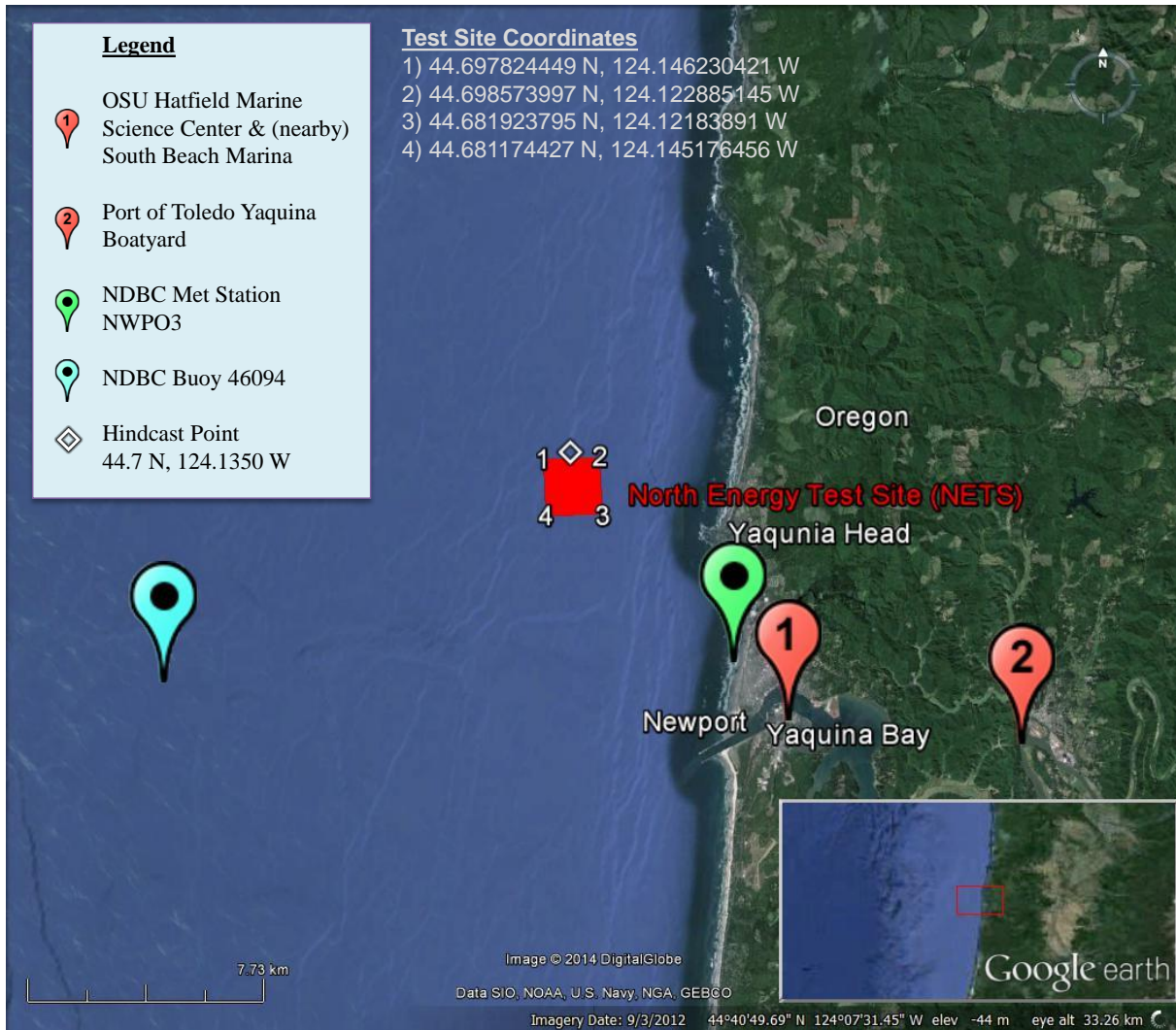


Figure 1: NETS is located in the coastal waters of Oregon near the City of Newport. The test site is 3-5 km off-shore in 45-55 m depth water. One National Data Buoy Center (NDBC) ocean buoy and one NDBC meteorological station are close to the site (see Table 1), as well as Oregon State University’s (OSU) test instrumentation buoy (see Section 3.2.7). The South Beach Marina, Port of Toledo Yaquina Boatyard, and OSU Hatfield Marine Science Center offer services valuable for WEC testing. The point of reference for the hindcast simulation is on the north edge of NETS. Image modified from Google Earth (Google Earth 2014).

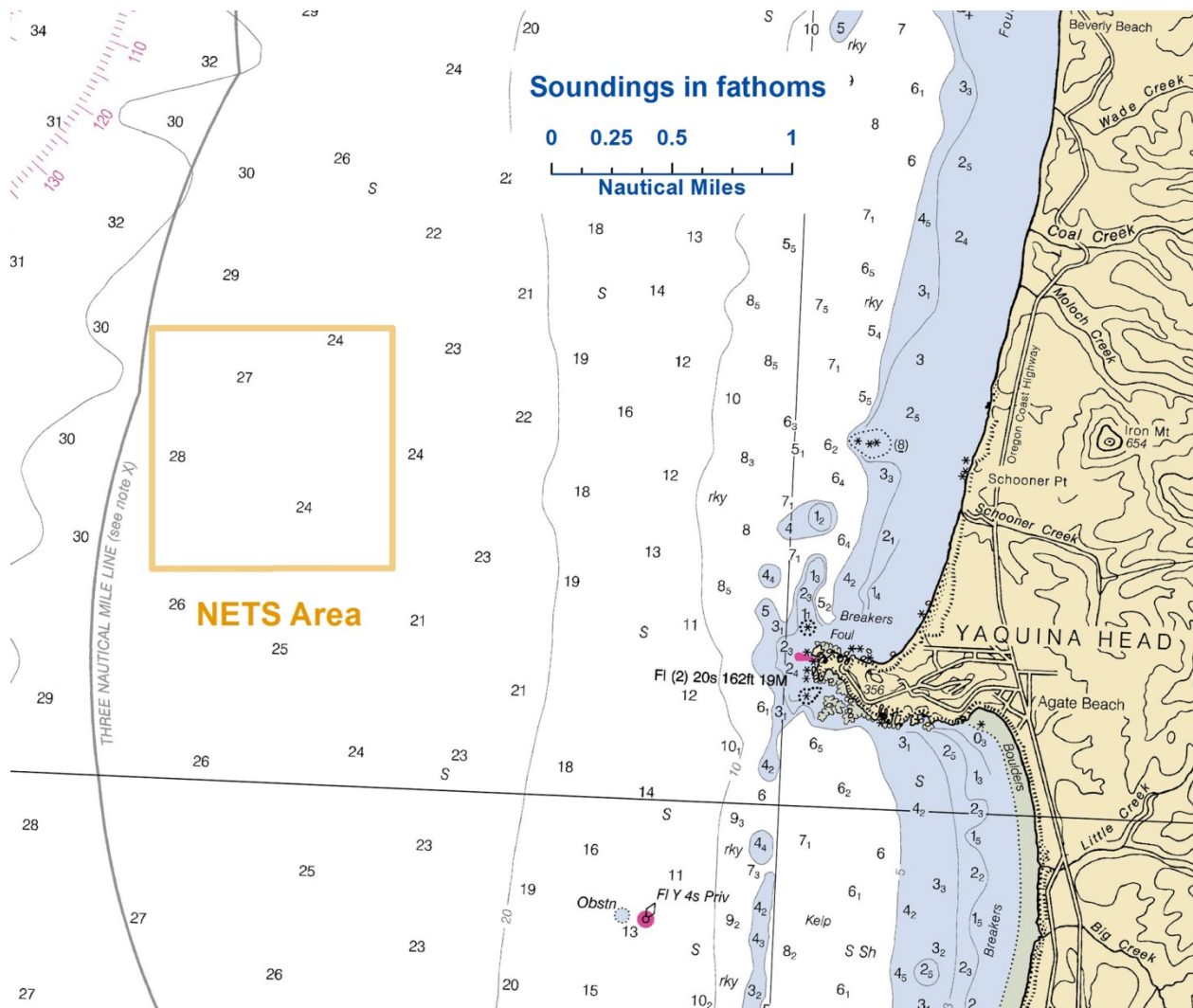


Figure 2: Nautical chart of Yaquina Head and surrounding area shows the gradually sloping bathymetry around NETS. Soundings in fathoms (1 fathom = 1.8288 m). Image modified from nautical chart #18561 (Office of Coast Survey 2011).

3.2. WEC Testing Infrastructure

3.2.1. Mooring Berths

NETS is permitted to test up to two WECs concurrently within the 45-55 m depth site. Mooring systems are not provided and would need to be installed according to the developers design. As an example, a six-point mooring system was used for the WET-NZ during their 2012 test. A layout of their test site mooring is provided in von Jouanne et al. (2013). A three point mooring system is used for OSU’s Ocean Sentinel buoy (described in Section 3.2.2) during device deployment in order to hold a tight watch circle along the device and to maintain the connection of the power and communication umbilical with the Ocean Sentinel (NNMREC 2014). During more energetic winter months, the Ocean Sentinel uses a single point mooring system and can be used for environmental testing, but will not be connected

to the device. WEC testing can be done in “stand alone” mode (no electrical connection) during the winter.

3.2.2. Electrical Grid Connection

There is no electrical grid connection at NETS, but the Ocean Sentinel test buoy (Figure 3) was designed as an electrical grid emulator to allow assessment of WEC device performance (von Jouanne et al. 2013). The Ocean Sentinel serves several purposes: (1) it consumes the electrical power generated by the WEC device with an onboard resistor element, (2) it measures the electrical power generated (voltage, current), and (3) it collects year-round met-ocean data, as described in Section 3.2.7.

The Ocean Sentinel can currently accommodate one device with an average power output up to 100 kW during the months May through October (NNMREC 2014). The data collected by the Ocean Sentinel is communicated wirelessly to OSUs Hatfield Maine Science Center, which is located in Yaquina Bay next to the South Beach Marina (Waypoint #1 in Figure 1). This data can be accessed remotely.

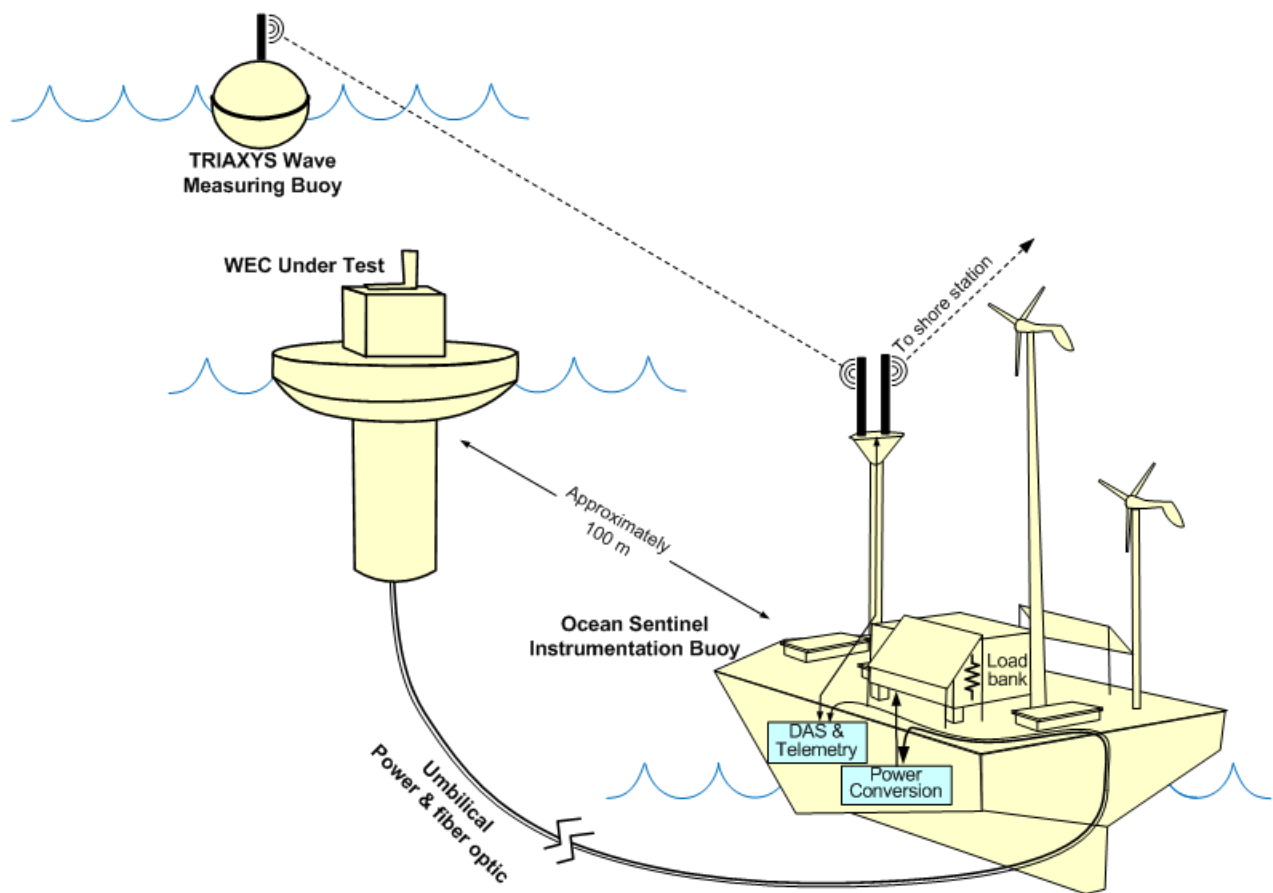


Figure 3: The Ocean Sentinel acts as a grid emulator for WEC devices, as well as records electricity output and monitors surrounding environmental data. The WEC device is connected to the Ocean Sentinel via an umbilical cord.

3.2.3. Facilitating Harbor

NETS is approximately 9 km north/northwest of the entrance to Yaquina Bay, the mouth of the Yaquina River. The South Beach Marina is located near the outlet of Yaquina Bay and offers year-round boat mooring (near Waypoint #1 in Figure 1).

3.2.4. On-Shore Office Space

The fishing and tourist City of Newport, Oregon, where approximately ten thousand people live, is on the north side of Yaquina Bay (U.S. Census Bureau 2012). At this time, developers at NETS are responsible for renting office space in Newport, Oregon or Toledo, Oregon, which is a town up the Yaquina River. Meeting rooms and temporary office space through P MEC are planned to be available in the future following the completion of the South Energy Test Site (SETS) (Batten 2014).

3.2.5. Service Vessel and Engineering Boatyard Access

No dedicated service vessel is available at this time, but following the completion of SETS, more resources may be available through P MEC. Service vessels for hire are likely available in the Newport/Toledo area. The Port of Toledo's Yaquina Boatyard (Waypoint #2 in Figure 1) services boats and provides space for self-service. Yaquina Boatyard hauls boats up to 300 tons and has capabilities that include steel fabrication, carpentry, painting, haul-out, and project management (Port of Toledo 2014).

3.2.6. Travel and Communication Infrastructure

Portland International Airport (PDX) is a two and a half hour drive from Newport, Oregon. Eugene Airport is located closer and is a one hour and forty minute drive. Cellular service offers consistent coverage; three Federal Communication Commission (FCC) registered cell phone towers are located in and around Newport, Oregon.

3.2.7. Met-Ocean Monitoring Equipment

The Ocean Sentinel test buoy reports environmental data (waves, currents and winds), and other signals from the installations onboard the WEC test device (NNMREC 2014). As with electrical power data, met-ocean data is communicated wirelessly to OSUs Hatfield Marine Science Center (Waypoint #1 in Figure 1) and is available for remote access.

In addition, there are two National Buoy Data Center (NDBC) buoys that measure and collect ocean data and one NDBC station reporting meteorological data (see Figure 1 for location). Instrument and data specifications for this monitoring equipment are summarized in Table 1. Buoy data is accessible online at the NDBC database. NDBC 46050 (Stonewall Bank) is located 30 km seaward from the test site and provides spectral wave data. NDBC 46094 (NH-10) is slightly closer to the site at only 14 km away and reports standard ocean

wave data (Figure 4(a)). The land based meteorological station is situated directly on the shoreline (Figure 4(b)).



Figure 4: (a) Moored buoy NDBC 46094 located 14 km southwest of the test site, (b) meteorological station NWPO3 on the coastline 8 km southeast of the test site (National Data Buoy Center 2014).

Table 1: Wave monitoring equipment in close proximity to NETS.

Instrument Name (Nickname)	NDBC Station 46094 (also called NH-10)	NDBC Station 46050 (Stonewall Bank)			NWPO3	
Type	Moored buoy	3-meter discus buoy			C-MAN station (MARS payload)	
Measured parameters	-std. met. data -continuous winds -sea surface temp, salinity, density -current measurements	-std. met. data -continuous winds -spectral wave density -spectral wave direction			-std. met. data -continuous winds	
Variables reported, including derived variables (Sampling interval)	<i>Std Met.:</i> WDIR WSPD BAR ATMP (10 min sampling period)	<i>Std Met.:</i> WDIR WSPD GST WVHT DPD APD PRES ATMP WTMP (1 hr sampling period)	<i>Contin. Winds:</i> WDIR WSPD GDR GST GTIME (10 min sampling period)	-Spectral Wave Density -Spectral Wave direction (1 hr sampling period)	<i>Std Met.:</i> WD WSPD GST BAR ATMP DEWP (1 hr sampling period)	<i>Contin. Winds:</i> WDIR WSPD GDR GST GTIME (10 min sampling period)
Location	directly west of Newport, 14 km southwest from NETS	20 nm (nautical miles, 1 nm = 1.852 km) directly west of Newport, 30 km west of NETS			on the shoreline, near Newport, 8 km southeast of NETS	
Coordinates	44.633 N 124.304 W (44°38'0" N 124°18'13" W)	44.639 N 124.534 W (44°38'20" N 124°32'2" W)			44.613 N 124.067 W (44°36'48" N 124°4'0" W)	
Depth	-depth: 81 m -air temp: 2.5 m above site -anemometer: 3 m above site	-depth: 128 m -air temp: 4 m above water -anemometer: 5 m above water -barometer: sea level -sea temp depth: 0.6 m below water			-site: 9.1 m above sea level -air temp: 6.4 m above site -anemometer: 9.4 m above site -barometer: 11 m above sea level	
Data Start	2/5/2007	-std met: 11/16/1991 -contin winds: 09/07/1997 -spect wave dens: 01/01/1996 -spect wave dir: 03/05/2008			-std met: 1/10/1985 -contin winds: 1/12/1997	
Data End	present; several winters missing data	present			present	
Period of Record	~8.5 yrs	-std met: ~24 yrs -contin winds: ~18 yrs -spect wave dens: ~20 yrs -spect wave dir: ~7.5 yrs			-std met: ~31 yrs -contin winds: ~19 yrs	
Owner / Contact Person	Oregon Coastal Ocean Observing System/ National Data Buoy Center	National Data Buoy Center			National Data Buoy Center	

3.2.8. *Environmental Monitoring*

Environmental conditions have been characterized at the site by Oregon State University, NOAA, and NNMREC. The information gathered includes baseline measurements of benthic habitat and organisms, marine mammal populations, electromagnetic fields (EMF), and acoustics (Batten 2013). Developers can contract with NNMREC to monitor environmental effects of WEC deployments during testing. Required environmental monitoring of WEC deployments includes acoustics, electromagnetic fields (EMF), benthic ecosystems, and opportunistic marine mammal observations.

3.2.9. *Permitting*

The site is fully permitted through the NEPA process, Department of State Lands, the U.S. Coast Guard, and the Army Corp of Engineers (NNMREC 2014). Developers interested in testing WECs at NETS are required to provide plans and present information to show compliance with test center standards and regulatory requirements. Each test requires its own permits for WEC testing in Oregon state waters. The approval process has been streamlined, but it should be noted that completed permit applications and supporting documentation should be submitted at least six months prior to the desired deployment site. More information can be found at NNMREC's website <http://nnmrec.oregonstate.edu/permitting-requirements>.

3.3. **Data used**

Researchers at the Northwest National Marine Renewable Energy Center (NNMREC) produced a 7 year hindcast dataset for the area offshore of Oregon (García-Medina et al. 2014) in order to complement the study of temporal and spatial variability in the wave resource over the Pacific Northwest region by Lenee-Bluhm et al.(2011). This dataset was used to calculate statistics of interest for the wave resource characterization at NETS. The hindcast data at the grid point on the north side of NETS was analyzed (see Figure 1). Although a 10 year hindcast would be preferred, García-Medina et al. (2014) showed that the probability density function (PDF) of significant wave height from their hindcast compared to NDBC 46029 buoy data were in agreement up to ~ 7 m, and, therefore, the hindcast is at least representative of the twenty-seven years of buoy operation, 1985 – 2011.

In addition to the hindcast data set, historical data from buoy NDBC 46050 was used to calculate extreme sea states and representative spectra. Wind data was available from NDBC 46050 and a Coastal-Marine Automated Network (C-MAN) station, NWPO3 located just on-shore. However, to be consistent with the other sites, Climate Forecast System Reanalysis (CFSR) winds were used, as explained in Section 2.3. As with the other sites, current data was downloaded from OSCAR. See Figures 1 and 5 for data locations.



Figure 5: NETS location map showing CSFR wind and OSCAR surface current data points, and NDBC buoy locations (Google Earth 2015).

3.4. Results

The following sections provide information on the joint probability of sea states, the variability of the IEC TS parameters, cumulative distributions, weather windows, extreme sea states, and representative spectra. This is supplemented by wave roses as well as wind and surface current data in Appendix A. The wind and surface current data provide additional information to help developers plan installation and operations & maintenance activities.

3.4.1. Sea States: Frequency of Occurrence and Contribution to Wave Energy

Joint probability distributions of the significant wave height, H_{m0} , and energy period, T_e , are shown in Figure 6. Figure 6 (top) shows the frequency of occurrence of each binned sea state and Figure 6 (bottom) shows the percentage contribution to the total wave energy. Figure 6 (top) indicates that the majority of sea states are within the range $1 \text{ m} < H_{m0} < 3.5 \text{ m}$ and $7 \text{ s} < T_e < 11 \text{ s}$; but a wide range of sea states are experienced at NETS, including extreme sea states caused by severe storms where H_{m0} exceeded 7.5 m. The site is well suited for testing WECs at various scales, including full-scale WECs, and testing the operation of WECs under normal sea states. Although the occurrence of an extreme sea state for survival testing of a full scale WEC is unlikely during a normal test period, the NETS wave climate offers opportunities for survival testing of scaled model WECs.

As mentioned in the methodology (Section 2.2), previous studies show that sea states with the highest frequencies of occurrence do not necessarily correspond to those with the highest contribution to total wave energy. The total wave energy in an average year is 322,250 kWh/m, which corresponds to an average annual omnidirectional wave power of 36.8 kW/m. The most frequently occurring sea state is within the range $1 \text{ m} < H_{m0} < 1.5 \text{ m}$ and $8 \text{ s} < T_e < 9 \text{ s}$, while the sea state that contributes most to energy is within the range $3 \text{ m} < H_{m0} < 3.5 \text{ m}$ and $10 \text{ s} < T_e < 11 \text{ s}$. Several sea states occur at a similar frequency, and sea states within $2 \text{ m} < H_{m0} < 4.5 \text{ m}$ and $9 \text{ s} < T_e < 11 \text{ s}$ contribute a similar amount to energy.

Frequencies of occurrence and contributions to energy of less than 0.01% are considered negligible and are not shown for clarity. For example, the sea state within $0.5 \text{ m} < H_{m0} < 1 \text{ m}$ and $5 \text{ s} < T_e < 6 \text{ s}$ has an occurrence of 0.02%. The contribution to total energy, however, is only 0.001% and, therefore, does not appear in Figure 6 (bottom). Similarly, the sea state within $8.5 \text{ m} < H_{m0} < 9 \text{ m}$ and $12 \text{ s} < T_e < 13 \text{ s}$ has an occurrence of 0.004%, but the contribution to total energy is 0.06%.

Curves showing the mean, 5th and 95th percentiles of wave steepness, H_{m0}/λ , are also shown in Figure 6. The mean wave steepness at NETS is 0.0165 ($\approx 1/61$), and the 95th percentile approaches 1/34.

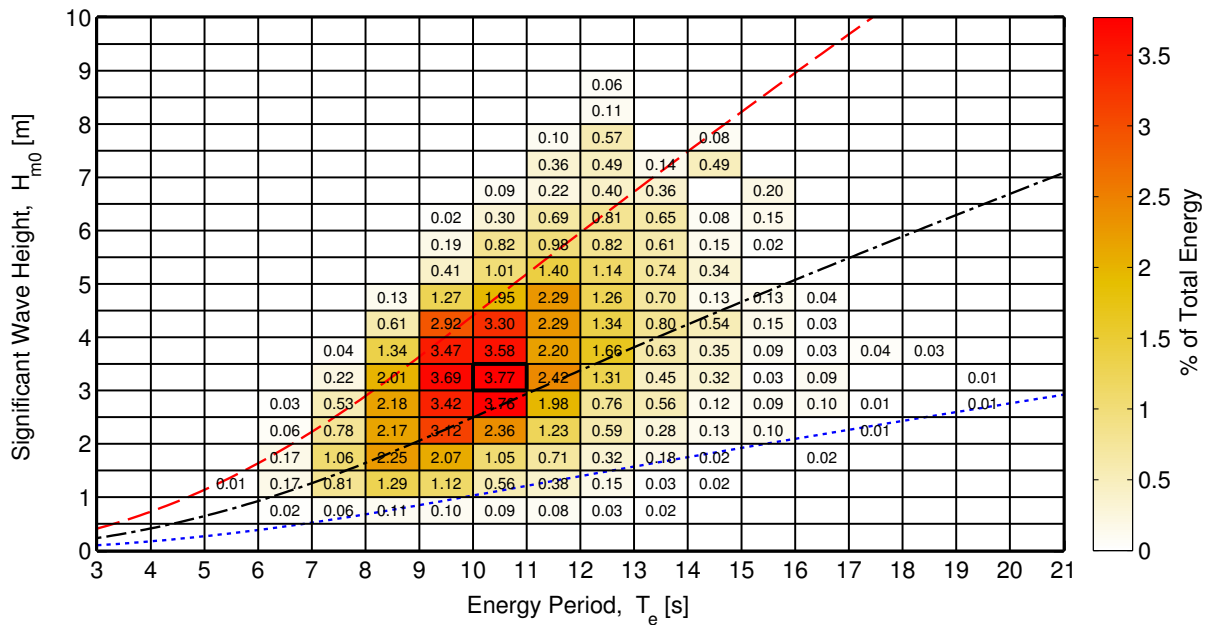
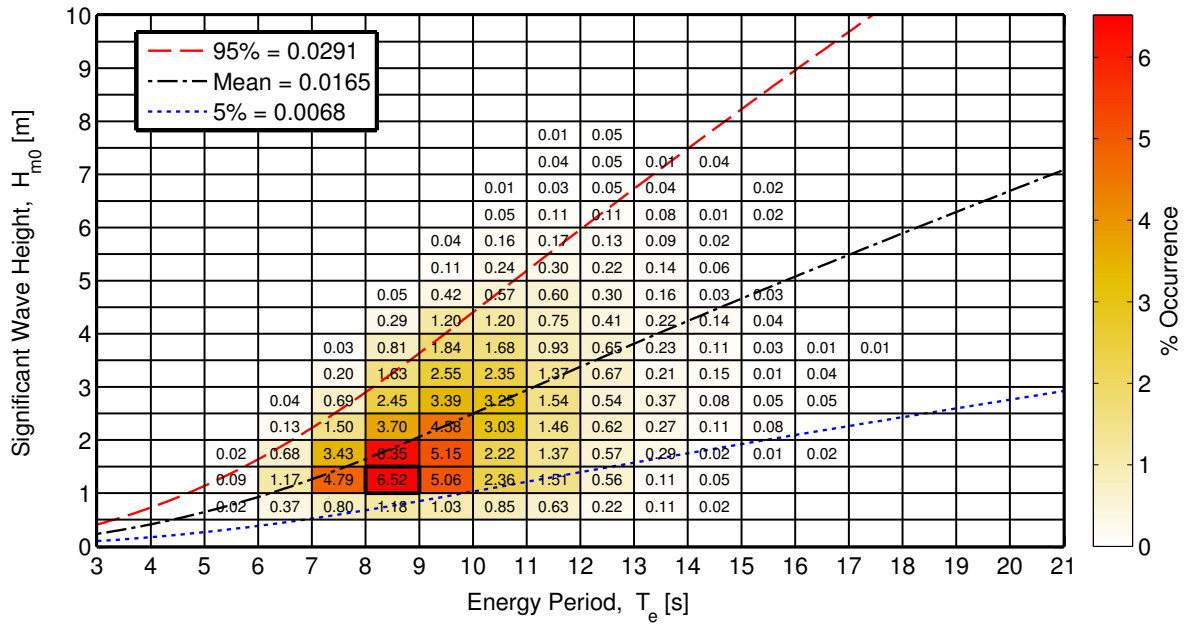


Figure 6: Joint probability distribution of sea states for NETS. The top figure is frequency of occurrence and the bottom figure is percentage of total energy, where total energy in an average year is 322,250 kWh/m.

3.4.2. IEC TS Parameters

The monthly means of the six IEC TS parameters, along with the 5th and 95th percentiles, are shown in Figure 7. The months, March – February, are labeled with the first letter (e.g., March is M). The values in the figure are summarized in Table 9 in Appendix A.

Monthly means of the significant wave height, H_{m0} , and the omnidirectional wave power density, J , show the greatest seasonal variability compared to the other parameters. Values are largest and vary the most during the winter months. The same trend is observed for the monthly mean energy period, T_e , but its variation is less pronounced. These observations are consistent with the relationship between wave power density, significant wave height and energy period, where wave power density, J , is proportional to the energy period, T_e , and the square of the significant wave height, H_{m0} .

Seasonal variations of the remaining parameters, ϵ_0 , θ_J , and d_θ , are much less than J , H_{m0} , and T_e , and are barely discernable. Monthly means for spectral width, ϵ_0 , remain nearly constant at ~ 0.4 . Similarly, monthly means for wave direction, θ_J , remains nearly constant from west at $\sim 275^\circ$, and directionality coefficient, d_θ , remains at ~ 0.9 . In summary, the waves at NETS, from the perspective of monthly means, have a fairly consistent spectral width, are predominantly from the west, and exhibit a wave power that has a narrow directional spread.

Wave roses of wave power and significant wave height, presented in Appendix A, Figure 120 and 121, also show the predominant direction of the wave energy at NETS, which is west, with frequent but small shifts to the north and occasional but small shifts to the south. Figure 120 shows two dominant wave direction sectors, west (at 270°) and west/northwest (WNW) at 285° . Along the predominant wave direction, 285° , the omnidirectional wave power density is at or below 35 kW/m about 24% of the time, but greater than 35 kW/m nearly 15% of the time. Along the west direction (270°), wave power density is at or below 35 kW/m about 18% of the time, and greater than 35 kW/m nearly 10% of the time.

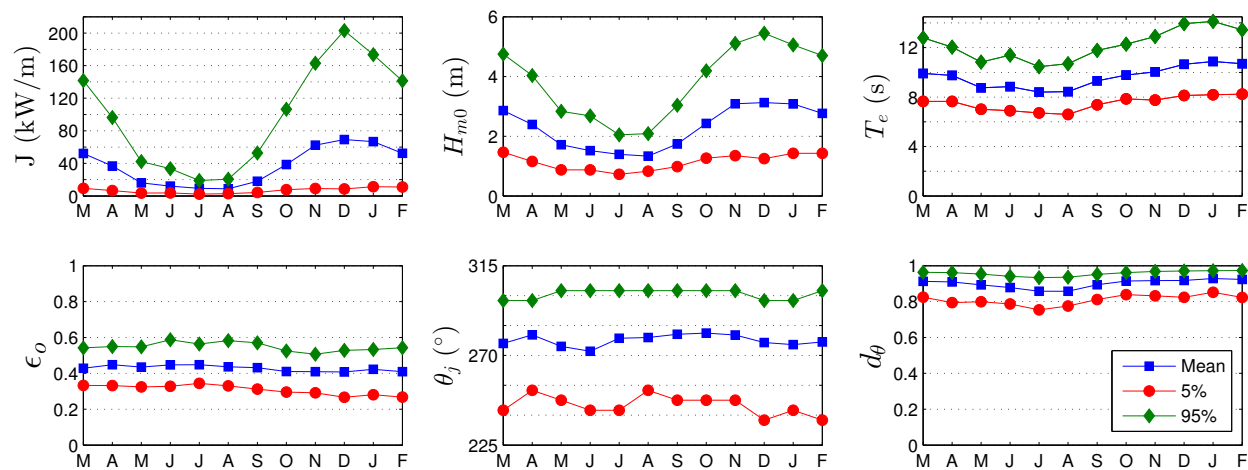


Figure 7: The average, 5th and 95th percentiles of the six parameters at NETS.

Monthly means, however, smear the significant variability of the six IEC parameters over small time intervals as shown in plots of the parameters at 1-hour intervals in Figure 8 for a representative year. While seasonal patterns described for Figure 7 are still evident, these plots show how sea states can vary abruptly at small time scales with sudden changes, e.g., jumps in the wave power as a result of a storm.

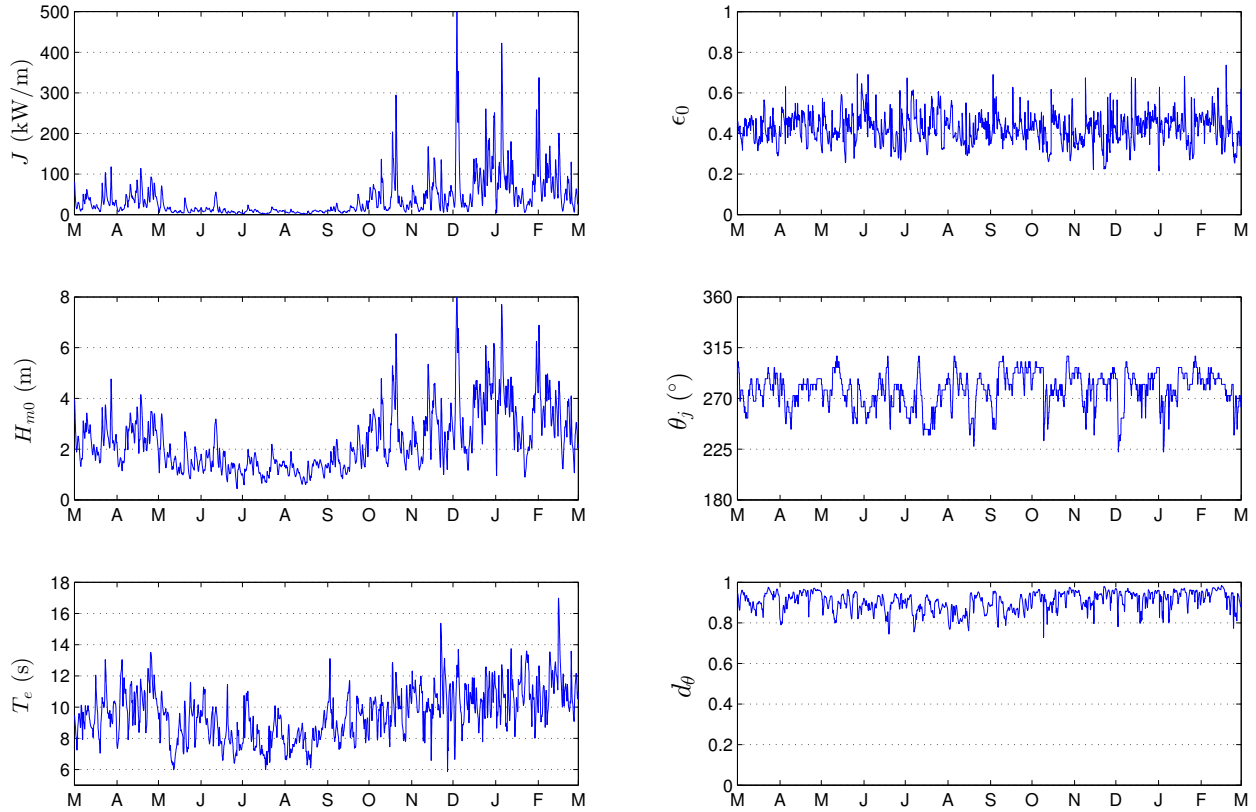


Figure 8: The six parameters of interest over a one-year period, March 2007 – February 2008 at NETS.

3.4.3. Cumulative Distributions

Annual and seasonal cumulative distributions (a.k.a., cumulative frequency distributions) are shown in Figure 9. Note that spring is defined as March – May, summer as June – August, fall as September – November, and winter as December – February. The cumulative distributions are another way to visualize and describe the frequency of occurrence of individual parameters, such as H_{m0} and T_e . A developer could use cumulative distributions to estimate how often they can access the site to install or perform operations and maintenance based on their specific device, service vessels, and diving operation constraints. For example, if significant wave heights need to be less than or equal to 1 m for installation and recovery, according to Figure 9, this condition occurs nearly 6% of the time on average within a given year. If significant wave heights need to be less than or equal to 2 m for emergency maintenance, according to Figure 9, this condition occurs about 49% of time on average within a given year. Cumulative distributions, however, do not account for the duration of a desirable sea state, or weather window, which is needed to plan deployment and servicing of a WEC device at a test site. This limitation is addressed with the construction of weather window plots in the next section.

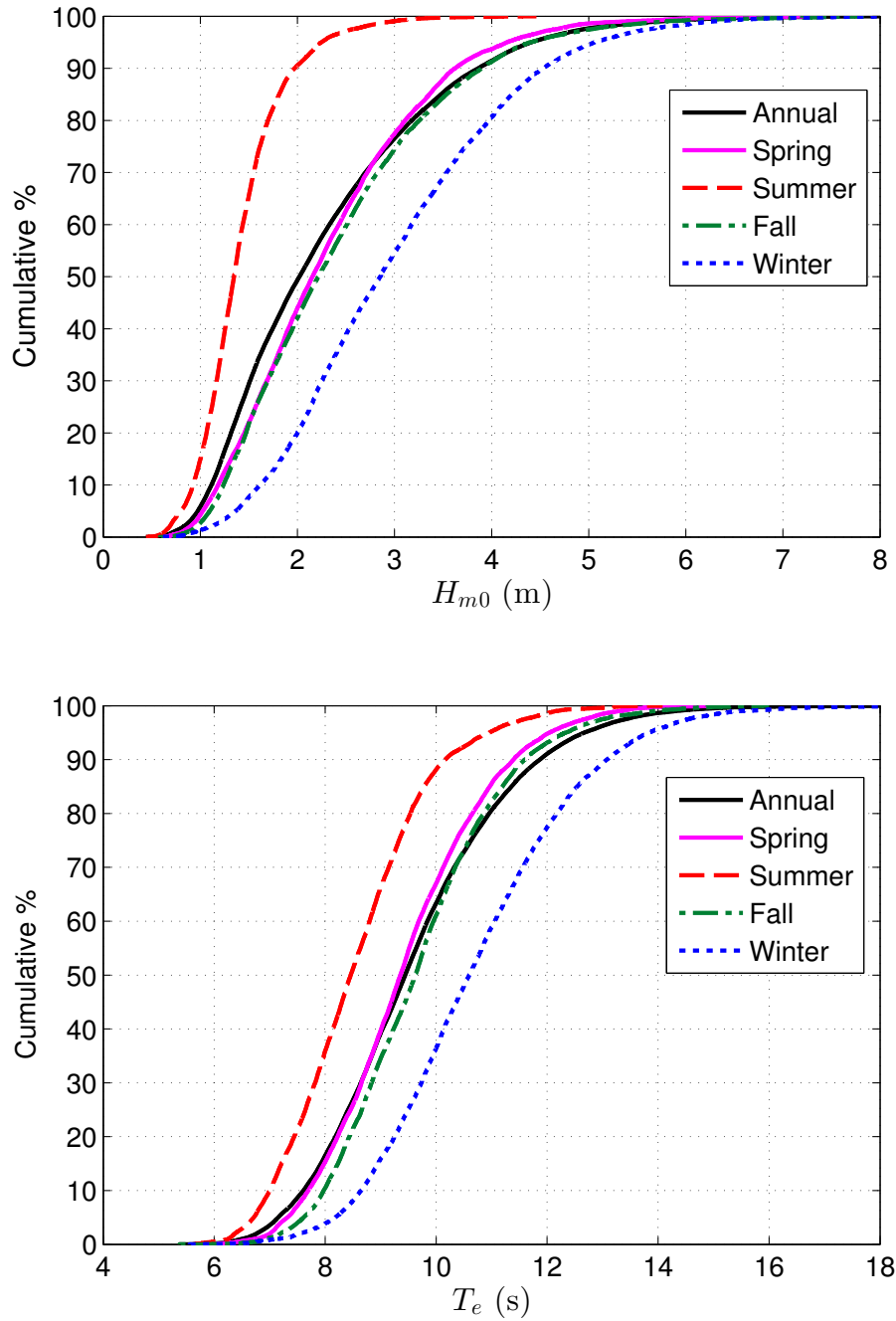


Figure 9: Annual and seasonal cumulative distributions of the significant wave height (top) and energy period (bottom) at NETS.

3.4.4. Weather Windows

Figure 10 shows the number of weather windows at NETS, when significant wave heights are at or below some threshold value for a given duration, for an average winter, spring, summer and fall. In these plots, each occurrence lasts a duration that is some multiple of 6-hours. The minimum weather window is, therefore, 6-hours in duration, and the maximum

is 96-hours (4 days). The significant wave height threshold is the upper bound in each bin and indicates the maximum significant wave height experienced during the weather window. Note that the table is cumulative, so, for example, an occurrence of $H_{m0} \leq 1$ m for at least 30 consecutive hours in the fall is included in the count for 24 consecutive hours as well. In addition, one 12-hour window counts would count as two 6-hour windows. It is clear that there are significantly more occurrences of lower significant wave heights during the summer than winter, which corresponds to increased opportunities for deployment or operations and maintenance.

Weather window plots provide useful information at test sites when planning schedules for deploying and servicing WEC test devices. For example, if significant wave heights need to be less than or equal to 1 m for at least 12 consecutive hours to service a WEC test device at NETS with a given service vessel, there would be, on average, twenty-three weather windows in the summer, but only one in the winter. When wind speed is also considered, Figure 11 shows the average number of weather windows with the additional restriction of wind speed, $U < 15$ mph. The local winds (which are not necessarily driving the waves) are used in these weather windows, and are given in Appendix A.4. That wind data was not available from the hindcast, so data from CFSR was used (see Section 2.3, Appendix A.4). For shorter durations (6- and 12-hour windows), daylight is necessary. Windows with $U < 15$ mph and only during daylight hours are shown in Figure 12. Daylight was estimated as 5am – 10pm Local Standard Time (LST).

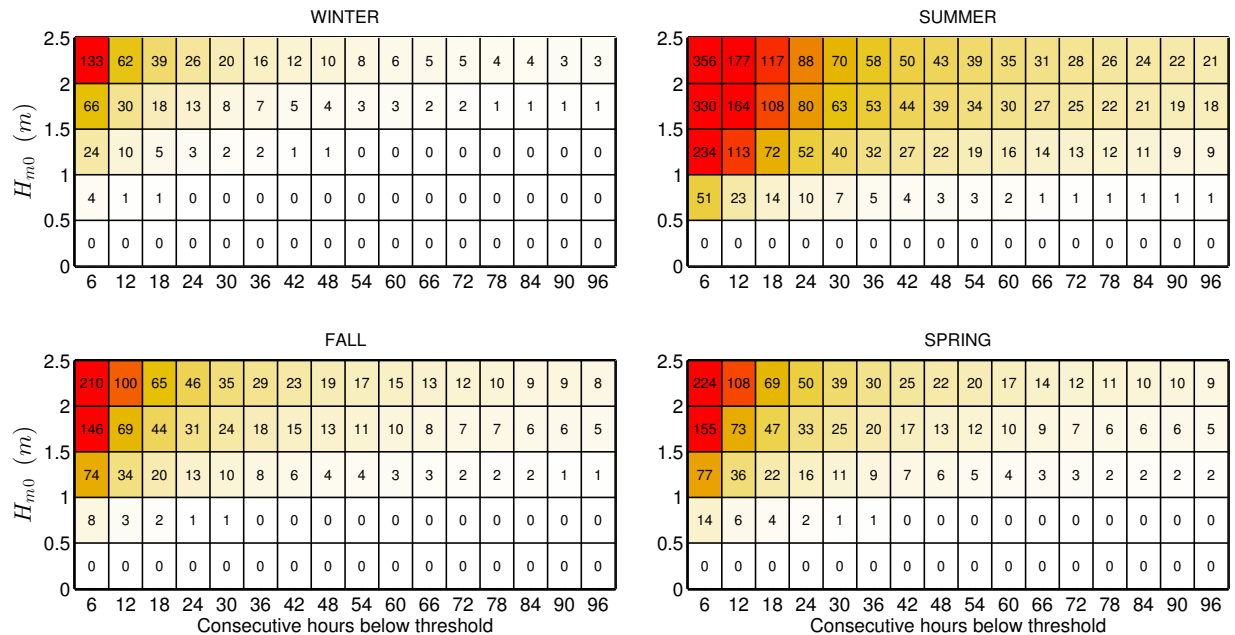


Figure 10: Average cumulative occurrences of wave height thresholds (weather windows) for each season at NETS. Winter is defined as December – February, spring as March – May, summer as June – August, and fall as September – November.

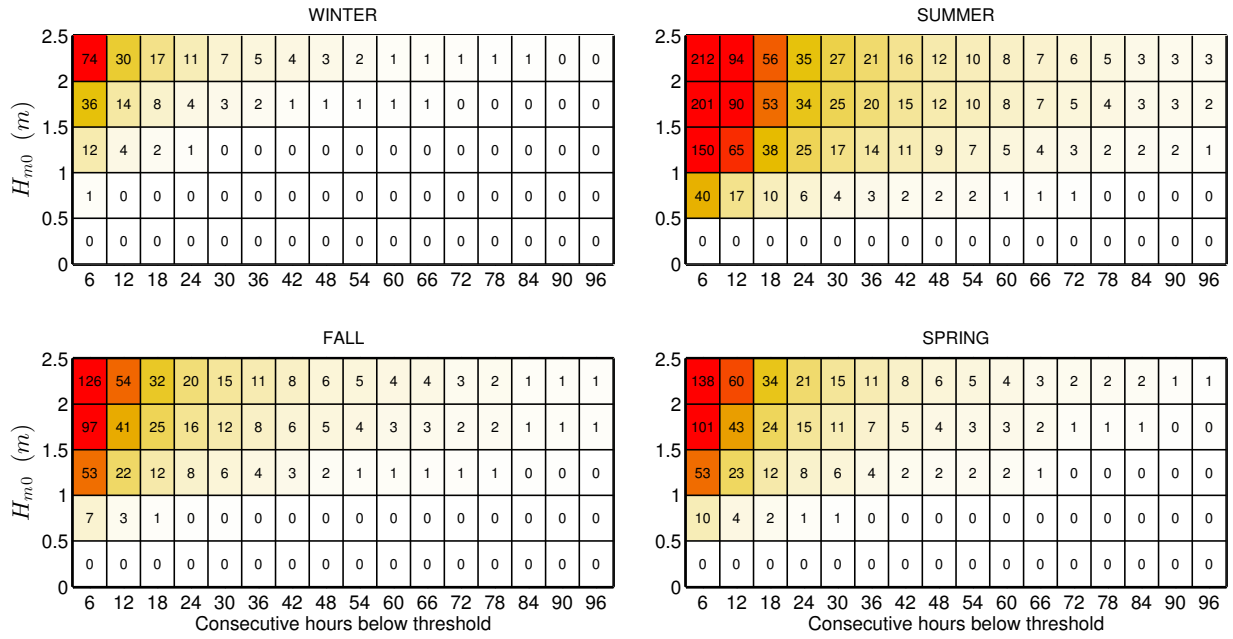


Figure 11: Average cumulative occurrences of wave height thresholds (weather windows) for each season at NETS with an additional restriction of $U < 15$ mph.

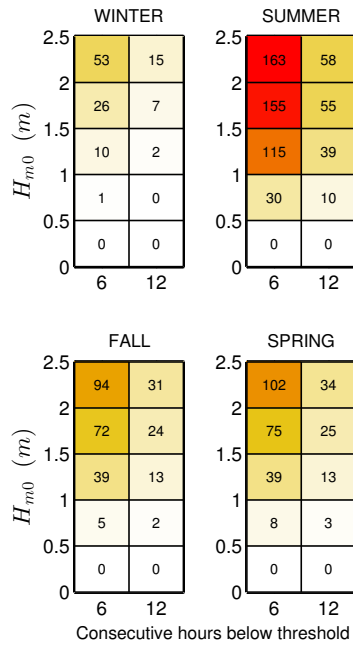


Figure 12: Average cumulative occurrences of wave height thresholds (weather windows) for 6- and 12-hour durations with $U < 15$ mph and only during daylight hours (5am – 10pm LST) at NETS.

3.4.5. Extreme Sea States

The modified IFORM was applied using NDBC 46050 data (see Table 1 for buoy information) to generate the 100-year environmental contour for NETS shown in Figure 13. Selected sea states along this contour are listed in Appendix A, Table 10. As stated in Section 1.2, environmental contours are used to determine extreme wave loads on marine structures and design these structures to survive extreme sea states of a given recurrence interval, typically 100-years. For NETS, the largest significant wave height estimated to occur every 100-years is over 17.3 m, and has an energy period of about 16.6 s. However, significant wave heights lower than 17.3 m, with energy period less than or greater than 16.6 s, listed in Table 10, could also compromise the survival of the WEC test device under a failure mode scenario in which resonance occurred between the incident wave and WEC device, or its subsystem. For comparison, 50- and 25-year return period contours are also shown in Figure 13. The largest significant wave height on the 50-year contour is 16.3 m with an energy period of about 16.4 s, and on the 25-year contour is 15.4 m and 16.1 s. It should be noted that conditions at the NDBC46050 buoy (at 128 m depth) may differ significantly from the conditions at the test site (at depths of 45-55 m).

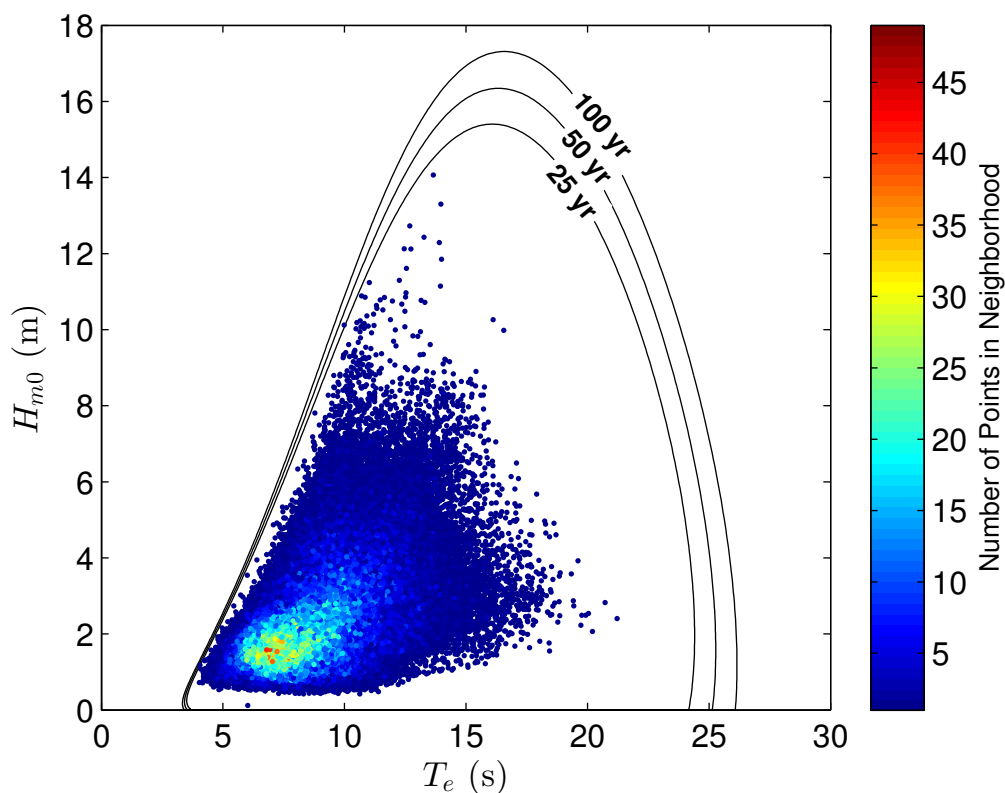


Figure 13: 100-year contour for NDBC 46050 (1996–2014).

3.4.6. Representative Wave Spectrum

All hourly discrete spectra measured at NDBC 46050 for the most frequently occurring sea states are shown in Figure 14. The most frequently occurring sea state, which is within the range $1.5 \text{ m} < H_{m0} < 2 \text{ m}$ and $7 \text{ s} < T_e < 8 \text{ s}$, was selected from a JPD similar to Figure 6 in Section 3.4.1, but based on the NDBC 46050 buoy data. As a result, the JPD, and therefore the most common sea states, generated from buoy data are slightly different from that generated from hindcast data. For example, the most frequently occurring sea state for the JPD generated from hindcast data is in a H_{m0} bin 0.5 m lower ($1 \text{ m} < H_{m0} < 1.5 \text{ m}$), and one second higher on bounds for T_e ($8 \text{ s} < T_e < 9 \text{ s}$). Often several sea states will occur at a very similar frequency, and therefore plots of hourly discrete spectra for several other sea states are also provided for comparison. Each of these plots includes the mean spectrum and standard wave spectra, including Bretschneider and JONSWAP, with default constants as described in Section 2.2.

For the purpose of this study, the mean spectrum is the ‘representative’ spectrum for each sea state, and the mean spectrum at the most common sea state, shown in Figure 14 (bottom-right plot), is considered the ‘representative’ spectrum at the site. The hourly spectra vary considerably about this mean spectrum, but this is partly reflective of the bin size chosen for H_{m0} and T_e . Comparisons of the representative spectra in all plots with the Bretschneider and JONSWAP spectra illustrate why modeled spectra with default constants, e.g., the shape parameter $\gamma = 3.3$ for the JONSWAP spectrum, should be used with caution. Using the constants provided in Section 2.2, the Bretschneider spectra are fair representations of the mean spectra in Figure 14, however it does not capture the bimodal nature of the spectra. The mean measured spectra is the best representation of the conditions, however, if these modeled spectra were to be used at this site, it is recommended that the constants undergo calibration against some mean spectrum, e.g., the representative spectrum constructed here. A better alternative may be to explore other methods or spectral forms to describe bimodal spectra (e.g., Mackay 2011) if it is known that the shape is not unimodal.

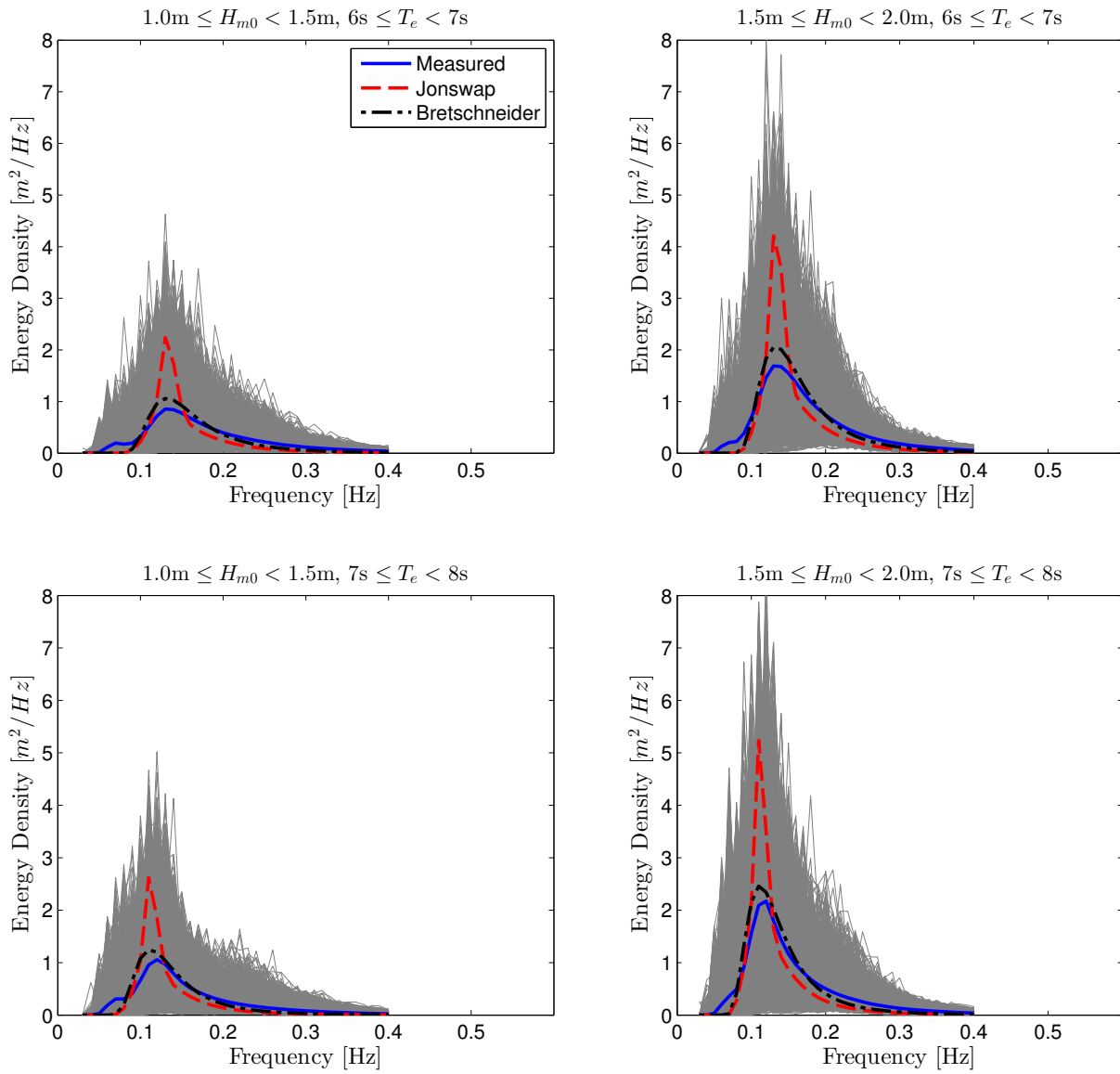


Figure 14: All hourly discrete spectra and the mean spectra measured at NDBC 46050 within the sea state listed above each plot. The JONSWAP and Bretschneider spectra are represented by red and black dotted lines, respectively.

4. U.S. NAVY WAVE ENERGY TEST SITE (WETS)

4.1. Site Description

The United States first grid-connected wave energy test site is being developed off the coast of the island of Oahu. The site, known as the U.S. Navy Wave Energy Test Site (WETS), is located on the windward side of the island at Marine Corps Base Hawaii (MCBH), at Kaneohe, as shown in Figure 15. The site infrastructure is being built by the U.S. Naval Facilities Engineering Command (NAVFAC) as a means of investigating the potential of wave energy to address the energy goals of the Navy. Through a cooperative effort between the Navy and the U.S. Department of Energy (DOE), the site will host companies seeking to test their pre-commercial WEC devices in an operational setting and advance their device transition readiness level. Now fully permitted and consisting of three berths, at water depths of 30 m (in place), 60 m, and 80 m (expected to be functional in 2016), all within about 2 km of shore, the site will be capable of hosting point absorber and oscillating water column WEC devices up to a peak power of 1 MW.

The site is located in Hawaiian state waters at approximately 21.47 N, 157.75 W (Figure 15). The deep water mooring sites overlay a featureless sandy substrate on a slightly steeper slope (Department of the Navy 2014). Figure 16 shows the bathymetry near Mokapu and the surrounding area. The wave climate at the test site is dominated by swells from the North Pacific, which are more frequent in the winter, and year-round waves formed by the northeast trade winds, which peak in the summer months between May-October (Department of the Navy 2014). The wave environment at WETS is characterized by an annual average power flux of 10–15 kW/m, with a significant number of events exceeding 40 kW/m each year. Despite this reliable wave energy, quiet periods are likely throughout the year, providing year round access to WEC devices.

NAVFAC operates the site and handles the permitted berths, grid connection infrastructure, device-specific permits, and offers office space. Typically a Cooperative Research and Development Agreement (CRADA) or a Navy contract is set up.

The Hawaii National Energy Institute at the University of Hawaii (HNEI-UH) is working with NAVFAC and DOE to support efforts at WETS in three key areas: (1) independent WEC device performance analysis; (2) environmental impact monitoring; and, (3) outfitting of a site-dedicated at-sea support platform. Environmental monitoring consists of ongoing measurements and analysis of the device acoustic signature, device and cabling electromagnetic fields (EMF), and possible changes in the device/mooring-induced sediment transport, seawater chemistry, and the ecological environment. HNEI will independently assess the device performance through robust wave environment measurements using Waverider buoys and an ADCP, wave forecast modeling, comprehensive device power output monitoring, the creation of power matrices to characterize performance as a function of wave state, and regular diver and ROV inspections of the deployed devices and associated mooring and cabling infrastructure. An additional UH effort is aimed at utilizing the data from WETS

to advance geophysical fluid dynamics-based models of device performance to guide design improvements, as well to advance ongoing efforts to improve WEC array modeling.

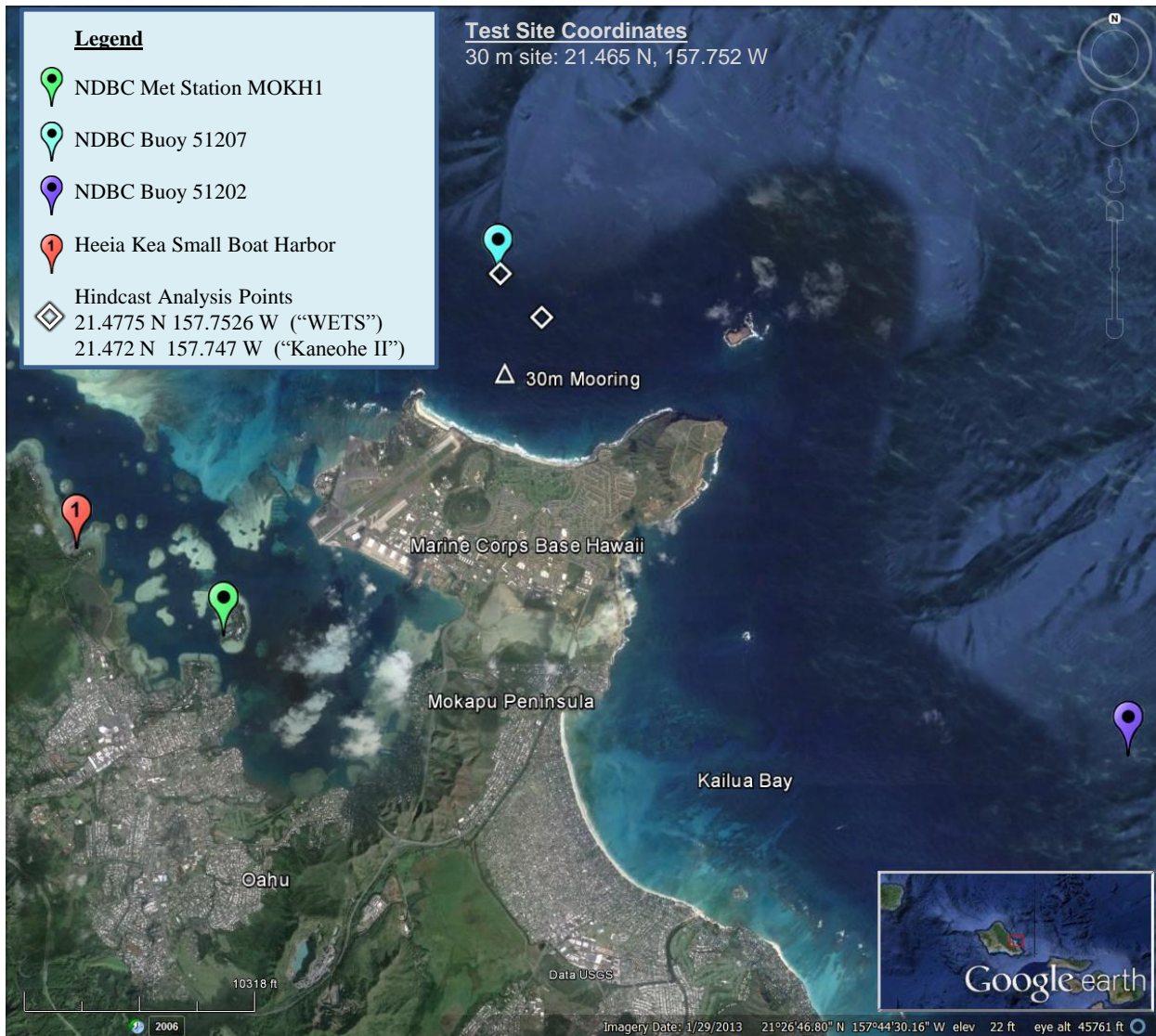


Figure 15: WETS is located on the northeast shore of Oahu, Hawaii near the Marine Corps Base Hawaii (MCBH). The site is 1–2 km off-shore in 30–80 m depth water and has one operational berth and two berths under construction. One National Data Buoy Center ocean buoy and one National Data Buoy Center meteorological station are close to the site (see Table 2). The Heeia Kea Small Boat Harbor is located in Kaneohe Bay and a boatyard is accessible in Honolulu, HI. The hindcast simulation used two points of reference as shown. Image modified from Google Earth (2014).

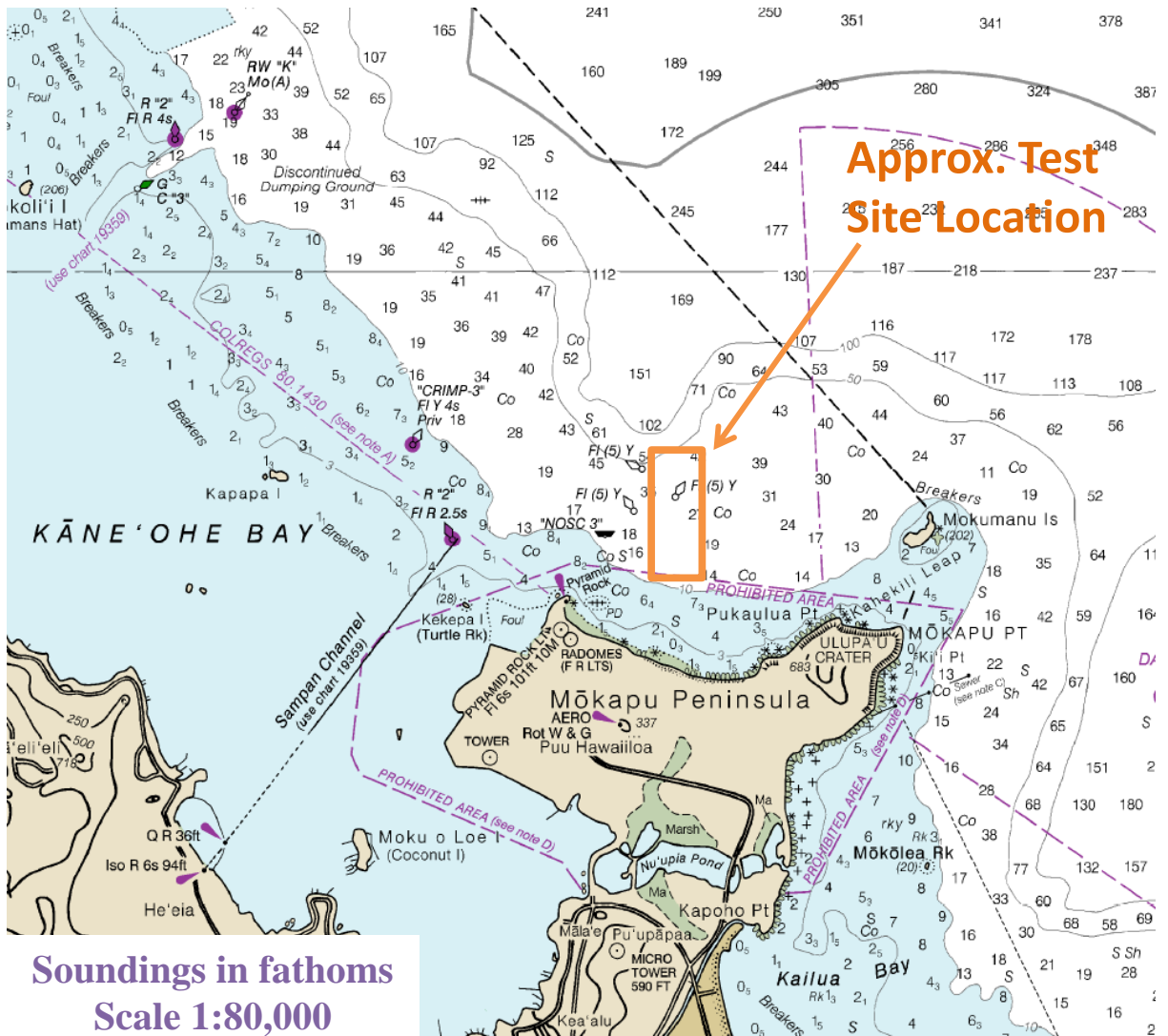


Figure 16: Nautical Chart of Mokapu Peninsula and surrounding area shows the gradually sloping bathymetry at WETS. Soundings in fathoms (1 fathom = 1.8288 m). Image modified from nautical chart #19357 (Office of Coast Survey 2013).

4.2. WEC Testing Infrastructure

4.2.1. Mooring Berths

There is one mooring berth at WETS and two under construction (Figure 17). The 30 m mooring berth uses a three point mooring system (a tri-moor configuration) with three sub-surface floats, two rock-bolted anchor bases and one gravity anchor. The mooring berth is fully functional and was used for testing a WEC device by Ocean Power Technologies between 2003 and 2011. Two deeper mooring berths at 60 m and 80 m are scheduled to be operational in 2016. They also employ three point mooring systems and each utilizes three surface floats and three drag embedment anchors, with the majority of the mooring system components provided by the Navy, including the anchor, ground change, mooring chain, and surface buoy. Figure 18 shows a schematic of one of the three mooring legs for the 60 m and 80 m berths which were designed by Sound & Sea Technology.

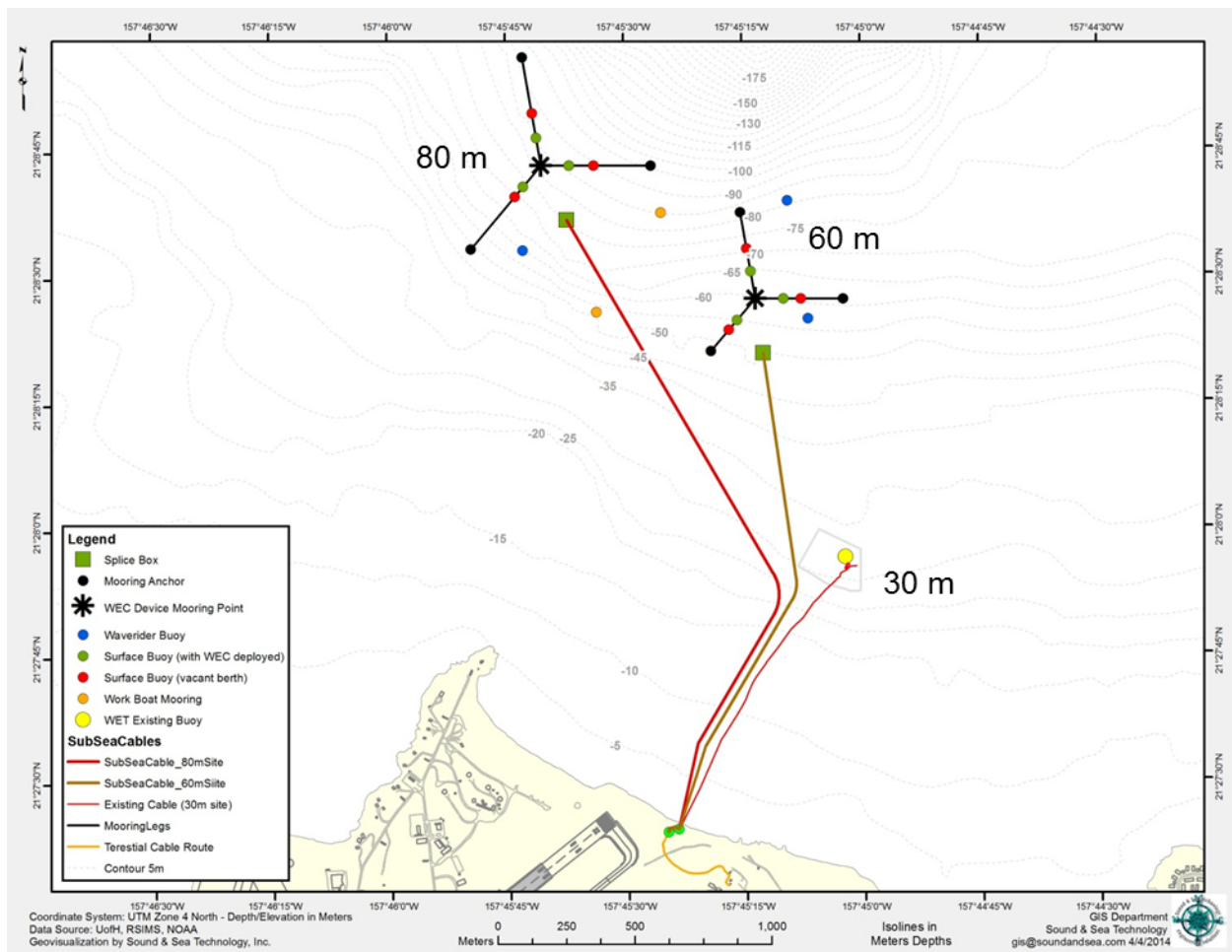


Figure 17: WETS mooring configuration and bathymetry map showing underwater cables and the three mooring sites at 30 m, 60 m, and 80 m depth (De Visser and Vega 2014).

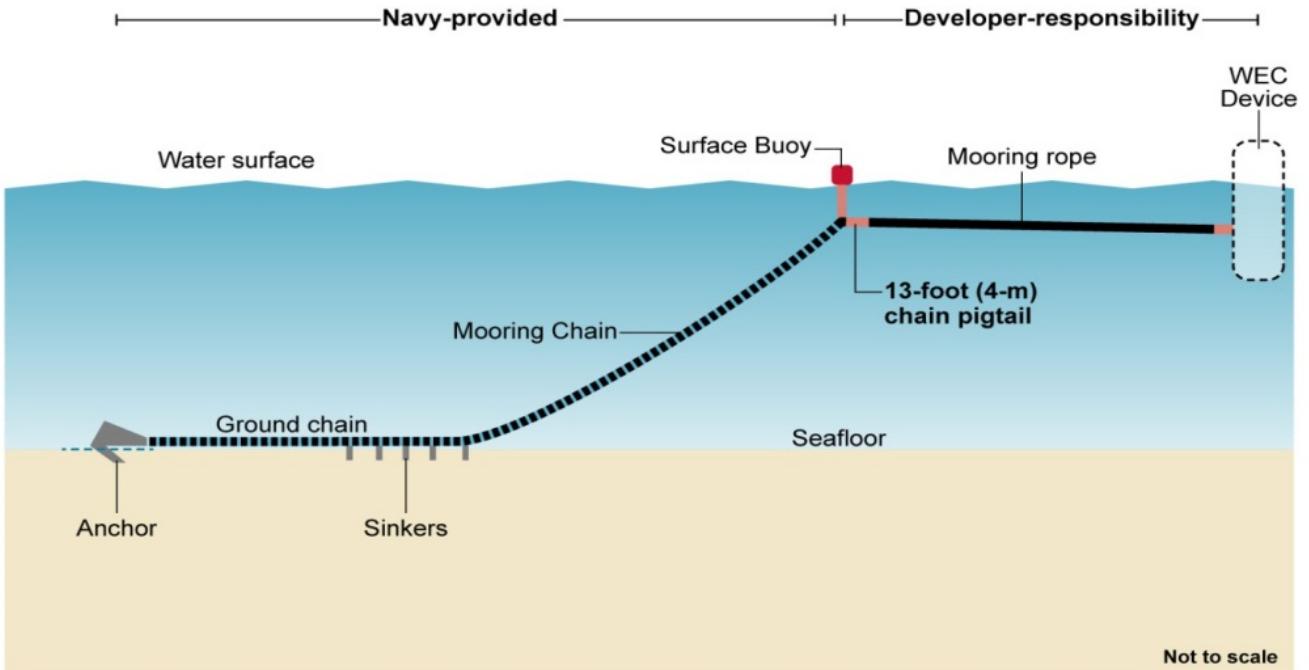


Figure 18: Sound & Sea Technology schematic of WETS 60 m and 80 m berths (De Visser and Vega 2014).

4.2.2. Electrical Grid Connection

WETS is a grid-accessible test site. An existing subsea cable with a maximum transmitting power of 250 kW at 4160 V services the 30 m mooring berth (De Visser and Vega 2014). Two additional cables are planned for installation by 2016 to service the 60 m and 80 m mooring berths and will transmit up to 1 MW at 11,500 V (De Visser and Vega 2014).

4.2.3. Facilitating Harbor

To the West and to the East of WETS is Kaneohe Bay and Kailua Bay, respectively, which are both popular recreation destinations. For boat mooring, the Heeia Kea Small Boat Harbor (Waypoint #1 in Figure 15) offers 54 moorings, 21 berths and 3 boat ramps (State of Hawaii Division of Boating and Ocean Recreation 2014).

4.2.4. On-Shore Office Space

WETS is 1–2 km offshore of the Marine Corps Base Hawaii (MCBH), which encompasses the area of Mokapu Peninsula. Office space is available through MCBH (De Visser and Vega 2014).

4.2.5. Service Vessel and Engineering Boatyard

A key focus at WETS, by the Navy, DOE, and HNEI, is reducing the considerable costs to developers associated with at-sea testing of WEC devices. The regular device and mooring inspections mentioned above are an important aspect of this. Additionally, HNEI plans to contract with a local ocean engineering company to provide a self-propelled barge equipped with cranes and hyperbaric chamber, dive and ROV facilities, an A-frame, and workspaces for WEC developers and UH scientists/engineers (Vega, 2014). To reduce mobilization costs and shorten emergency response time, this platform will be kept at Heeia Kea Small Boat Harbor, a state marina within an hours transit from the site. Further, a limited amount of emergency maintenance response will be provided to tenants at WETS, furthering HNEI's ability to fully document device reliability issues and develop operational and maintenance protocols for DOE and the Navy. In addition, several engineering boatyards are available in Honolulu Harbor with a variety of services available (Vega 2014).

4.2.6. Travel and Communication Infrastructure

The Honolulu International Airport is only a half hour drive from MCBH. Cellular phone coverage is adequate and consistent, and cell phones may be used on MCBH.

4.2.7. Met-Ocean Monitoring Equipment

Real-time meteorological and wave data are collected by two met-ocean buoys from the CDIP database, one on-shore meteorological station available through the Automated-Surface-Observing-System (ASOS) and one maintained by NOAA. Instrument and data specifications for this monitoring equipment are summarized in Table 2. Buoy data is accessible online at the CDIP databases. CDIP198 (NDBC 51207) (Figure 19 (a)) is located very close to the 80 m depth berth, and CDIP098 (NDBC 51202) (Figure 19 (b)) is located approximately 12 km southeast. On-shore, there is a meteorological station on MCBH near the site.



Figure 19: a) CDIP198 Waverider, b) CDIP098 Waverider (Coastal Data Information Program 2013).

Table 2: Wave monitoring equipment in close proximity to WETS.

Instrument Name (Nickname)	CDIP198/ NDBC 51207		CDIP198/ NDBC 51202 (Mokapu Point, HI)		ASOS PHNG Kaneohe Bay Marine Corps Airfield	MOKH1 - 1612480 Mokuoloe, HI
Type	Waverider Buoy		Waverider Buoy		Meteorological Station	Water Level Observation Network
Measured parameters	-std. met. data -spectral wave density data -spectral wave direction data		-std. met. data -spectral wave density data -spectral wave direction data		-wind dir & speed -barometric pressure -air temp -humidity	-wind dir & speed -gust -atmos press -air temp -water temp
Variables reported (includes derived variables)	<i>Std. Met.:</i> WVHT DPD APD MWD WTMP (30 min sampling period)	-Spectral Wave Density Spectral Wave direction (30 min sampling period)	<i>Std. Met.:</i> WVHT DPD APD MWD WTMP (30 min sampling period)	-Spectral Wave Density Spectral Wave direction (30 min sampling period)	WDIR WSPD (10 min sampling period) PRES ATMP 1 hour sampling period)	WDIR WSPD GST PRES ATMP WTMP (6 min sampling period)
Location	at WETS		directly east of Kailua Bay, 12 km southeast of WETS		Installed at MCBH, near the test site	on Coconut Island farther west into Kaneohe Bay than WETS)
Coordinates	21.477 N 157.753 W (21°28'39" N 157°45'10" W)		21.417 N 157.668 W (21°25'1" N 157°40'4" W)		unknown	21.432 N 157.790 W (21°25'55" N 157°47'24" W)
Depth	81 m		82 m		unknown	-air temp height: 5.5 m above site elevation -anemometer height: 12.7 m above site elevation -barometer elev: 2.8 m above mean sea level
Data Start	10/27/2012		8/10/2000		unknown	6/25/2008
Data End	present		present		present	present
Period of Record	~3 yrs		~15 yrs		unknown	~7 yrs
Owner/Contact Person	Pacific Islands Ocean Observing System (PacIOOS) – “Data provided by Scripps” Data reported at http://cdip.ucsd.edu/?ximg=search&xsearch=198&xsearch._Dtype=Station_I		Pacific Islands Ocean Observing System (PacIOOS) – “Data provided by Scripps” Data reported at http://cdip.ucsd.edu/?ximg=search&xsearch=098&xsearch._type=Station_ID		http://www.aviationweather.gov/metar	NOAA Tides & Currents

4.2.8. *Environmental Monitoring*

Environmental conditions at WETS have been characterized by the Navy with support from HNEI. Background environmental data includes wave, current, and climate data, as well as bathymetry and sediment profiles (De Visser and Vega 2014). Environmental monitoring, provided by HNEI, consists of ongoing measurements and analysis of acoustics, electromagnetic fields (EMF), and ecological surveys (to determine possible changes in sediment transport, seawater chemical composition, and the ecological environment).

4.2.9. *Permitting*

The berths at the site are permitted for testing of generic point absorbers and oscillating water column (OWC) devices. Developers must individually complete device-specific categorical exclusion applications, and an Army Corp of Engineers permit.

4.3. **Data Used**

Researchers affiliated with the Hawaii National Marine Renewable Energy Center (HINM-REC) at the University of Hawaii produced a 34 year hindcast dataset for the area offshore of Oahu (Li and Cheung 2014, Li et al. 2015). This hindcast is an improved version of that by Stopa et al. (2013). The 34 year dataset was used to calculate statistics of interest for the characterization. Note in Version 1 of this catalogue, only 10 years of the hindcast was available so data is updated to the full 34 years here. The hindcast data at two grid points (21.472 N, 157.747 W and 21.4775 N, 157.7526 W) for the 60 m “Kaneohe II” and 80 m “WETS” berths, respectively, were analyzed by UH (see Figure 15 and Figure 17 for location).

In addition to the hindcast data set, historical data from buoy NDBC 51202 was used to calculate estimates of extreme events because of its longer period of record (2001-2014). Historical data from buoy CDIP198/NDBC 51207 was used to calculate representative spectra because of its location at WETS. Wind data from CFSR was used, as explained in Section 2.3. A high resolution wind data set for the Hawaiian Islands (in addition to the global CFSR data set) was utilized in the hindcast by Li and Cheung (2014), and therefore monthly averages will be provided in Appendix B as well. As with the other sites, current data was downloaded from OSCAR. See Figures 15 and 20 for data locations.

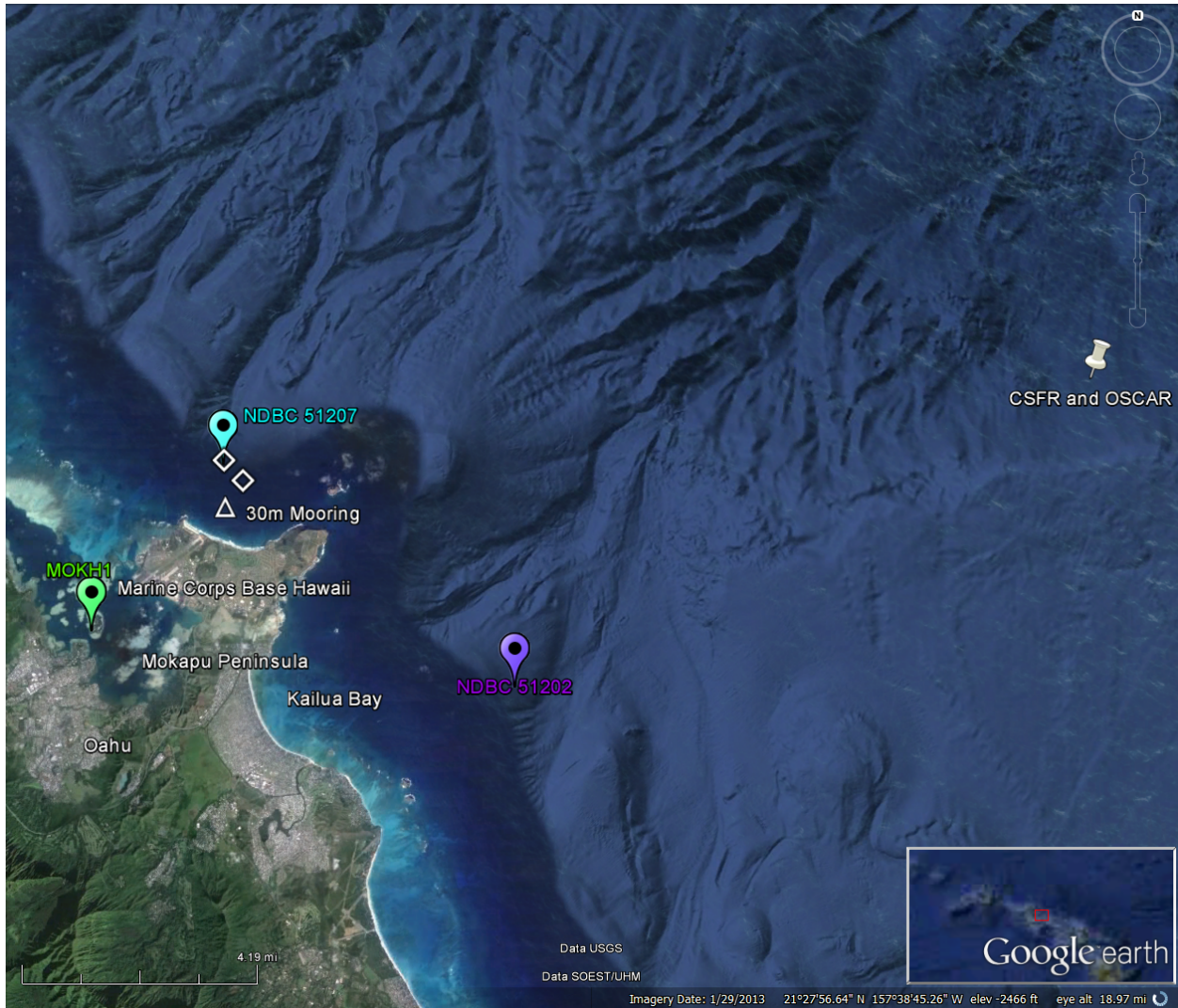


Figure 20: Two wave buoys and one met station surround the test site. The data points for OSCAR and CSFR overlap at 21.5 N, 157.5 W (Google Earth 2014).

4.4. Results

The following sections provide information on the joint probability of sea states, the variability of the IEC TS parameters, cumulative distributions, weather windows, extreme sea states, and representative spectra. This is supplemented by wave roses as well as wind and surface current data in Appendix B. The wind and surface current data provide additional information to help developers plan installation and operations & maintenance activities.

4.4.1. Sea States: Frequency of Occurrence and Contribution to Wave Energy

Joint probability distributions of the significant wave height, H_{m0} , and energy period, T_e , are shown in Figures 21 and 22. Figure 21 (top) shows the frequency of occurrence of each binned sea state and Figure 21 (bottom) shows the percentage contribution to the total

wave energy for “Kaneohe II” berth (60 m depth). The same information is shown for the “WETS” berth (80 m depth) in Figure 22. Figure 21 (top) and Figure 22 (top) indicate that the majority of sea states are within the range $1 \text{ m} < H_{m0} < 2.5 \text{ m}$ and $5 \text{ s} < T_e < 11 \text{ s}$. WETS experiences a minimal amount of extreme sea states, which rarely exceed 5 m. The site is well suited for testing WECs at various scales, and testing the operation of WECs under normal sea states. Year-round testing occurs at WETS and the winter storms may be considered for survival testing for scaled devices (compared to a full-scale devices deployed in a higher energy location).

As mentioned in the methodology (Section 2.2), previous studies show that sea states with the highest occurrence do not necessarily correspond to those with the highest contribution to total wave energy, as is the case in Figure 21 and Figure 22. The total wave energy in an average year is 114,450 kWh/m at the Kaneohe II berth and 125,850 kWh/m at the WETS berth, which corresponds to an average annual omnidirectional wave power of 13.0 kW/m and 14.3 kW/m. The most frequently occurring sea state is within the range $1 \text{ m} < H_{m0} < 1.5 \text{ m}$ and $6 \text{ s} < T_e < 7 \text{ s}$ for Kaneohe II, and $1.5 \text{ m} < H_{m0} < 2 \text{ m}$ and $6 \text{ s} < T_e < 7 \text{ s}$ for WETS, while the sea state that contributes most to energy is within the range $1.5 \text{ m} < H_{m0} < 2 \text{ m}$ and $7 \text{ s} < T_e < 8 \text{ s}$ for both Kaneohe II and WETS. Several sea states occur at a similar frequency, and sea states within $1 \text{ m} < H_{m0} < 2 \text{ m}$ and $6 \text{ s} < T_e < 8 \text{ s}$ contribute a similar amount to energy.

Frequencies of occurrence and contributions to energy of less than 0.01% are considered negligible and are not shown for clarity. For example, the sea state within $0.5 \text{ m} < H_{m0} < 1 \text{ m}$ and $13 \text{ s} < T_e < 14 \text{ s}$ has an occurrence of 0.01%. The contribution to total energy, however, is only 0.007% and, therefore, does not appear in Figure 21 (bottom). Similarly, the sea state within $3 \text{ m} < H_{m0} < 3.5 \text{ m}$ and $16 \text{ s} < T_e < 17 \text{ s}$ has an occurrence of 0.003%, but the contribution to total energy is 0.02%.

Curves showing the mean, 5th and 95th percentiles of wave steepness, H_{m0}/δ , are also shown in Figure 21 and Figure 22. The mean wave steepness is 0.0175 ($\approx 1/57$) at Kaneohe II and 0.0186 ($\approx 1/54$) at WETS. The 95th percentile is 0.0287 ($\approx 1/35$) at Kaneohe II and 0.0303 ($\approx 1/33$) at WETS.

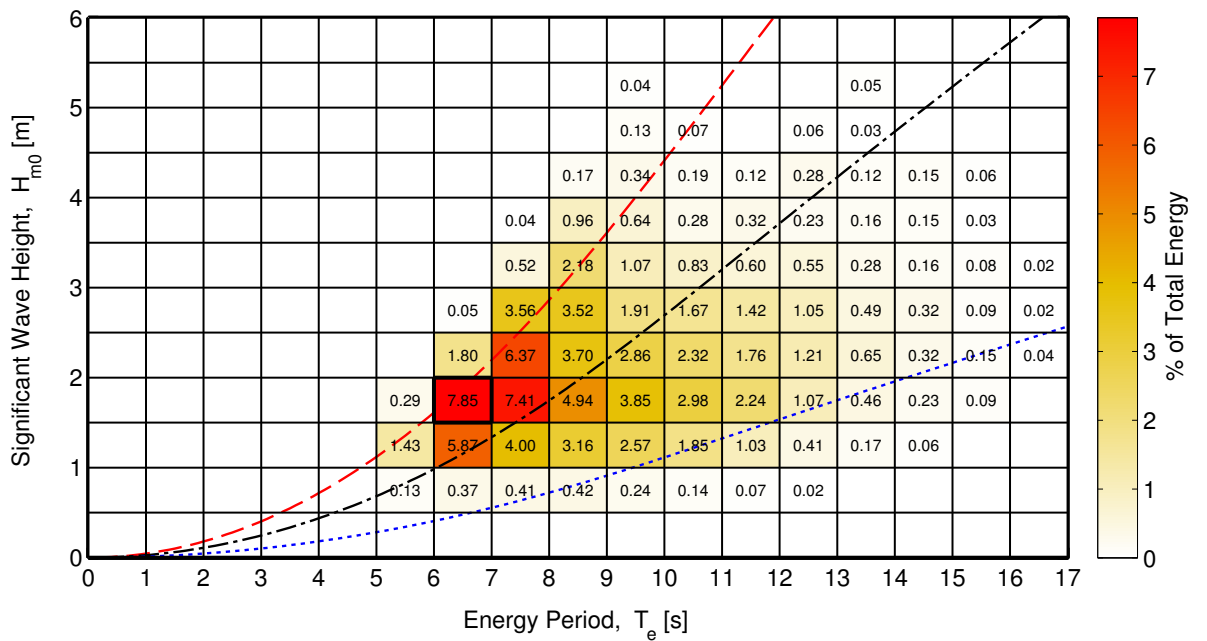
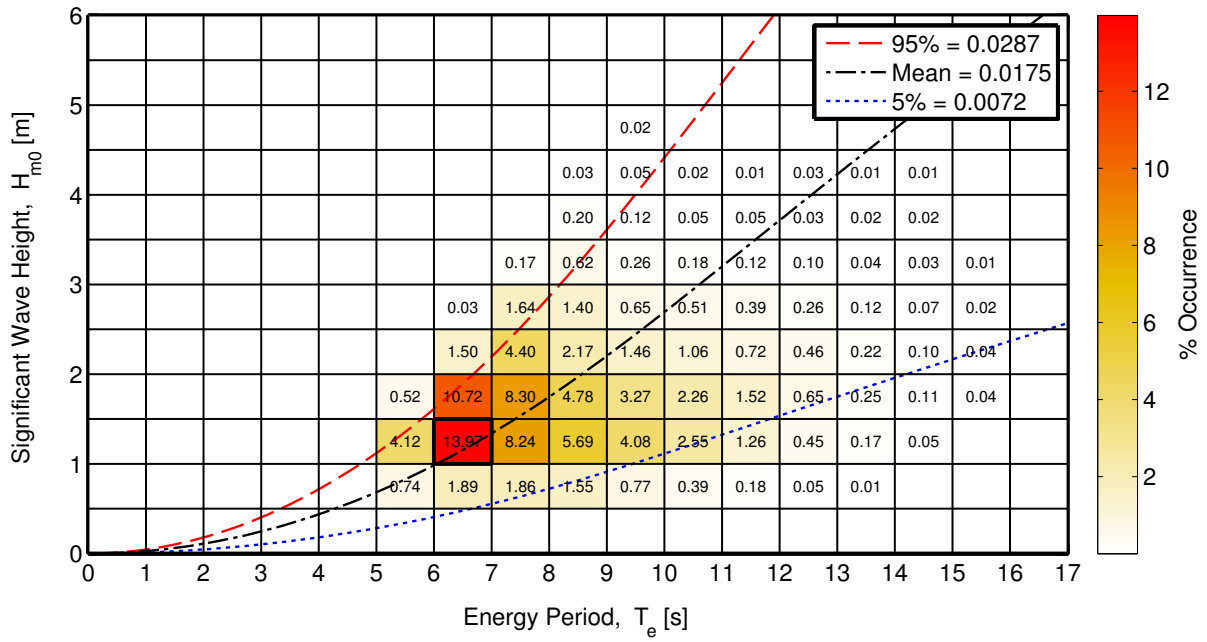


Figure 21: Joint probability distribution of sea states for the Kaneohe II berth (60 m depth). The top figure is frequency of occurrence and the bottom figure is percentage of total energy, where total energy in an average year is 114,450 kWh/m.

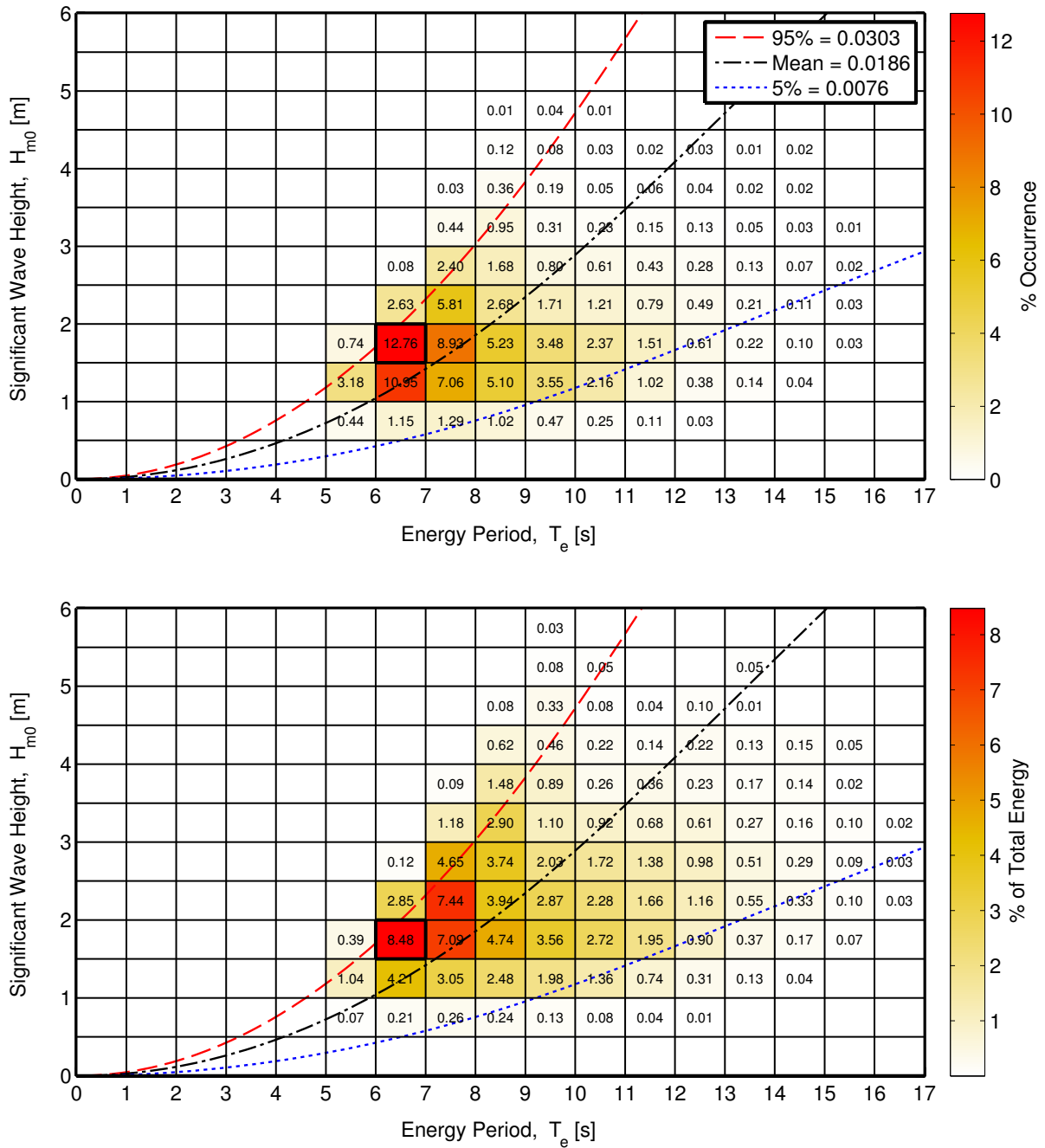


Figure 22: Joint probability distribution of sea states for the WETS berth (80 m depth). The top figure is frequency of occurrence and the bottom figure is percentage of total energy, where total energy in an average year is 125,850 kWh/m.

4.4.2. IEC TS Parameters

The monthly means of the six IEC TS parameters, along with the 5th and 95th percentiles, are shown in Figures 23 and 24. The values in the figures are summarized in Tables 13 and 14 in Appendix B.

Monthly means of the omnidirectional wave power, J , significant wave height, H_{m0} , and energy period, T_e , show the greatest seasonal variability compared to the other parameters. Values are largest and vary the most during the winter months. These observations are consistent with the relationship between wave power density, significant wave height and energy period, where wave power density, J , is proportional to the energy period, T_e , and the square of the significant wave height, H_{m0} .

The directionality coefficient (larger values indicate low directional spreading), is slightly larger in the summer, and it can be seen that the direction of maximum directionally resolved wave power (defined as the direction from which waves arrive in degrees clockwise from north), is most consistently from north/northeast during the summer, and varies more throughout the rest of the year. This is because summer months are dominated by wind waves from the northeast, while the winter months are made up of both wind waves and frequent swells from the North Pacific.

Seasonal variation of the spectral width, ϵ_0 , is much less than the other parameters and barely discernable. Monthly means for ϵ_0 remain nearly constant between 0.35 and 0.4. In summary, the waves at both the Kaneohe II and WETS berths, from the perspective of monthly means, have a fairly consistent spectral width, are predominantly from the north/northeast, and exhibit a wave power that has a fairly narrow directional spread in the summer, and a wider directional spread in the winter.

Wave roses of wave power and significant wave height, presented in Appendix B, Figure 126 and Figure 127, also show the spread of direction of the maximum wave energy at WETS. The larger waves (with higher wave power), often come as swells from the North Pacific, while smaller waves usually come from the northeast as wind waves. Figure 126 shows two dominant wave direction sectors, northeast and approximately east-northeast (ENE). Along the predominant wave direction, which is northeast (45°), the omnidirectional wave power density is at or below 35 kW/m less than 25% of the time, and greater than 35 kW/m approximately 1-2% of the time. Along the ENE direction (60°), wave power density is at or below 35 kW/m about 25% of the time and rarely (about 1% of the time) exceeds 35 kW/m.

Note that the wave climate is made up of swells from the North and South Pacific and year-round wind waves from the northeast. Therefore the direction of maximum directionally resolved wave power may not fully describe the origin of the wave power (i.e., the combination of swells and year-round wind waves from slightly different directions).

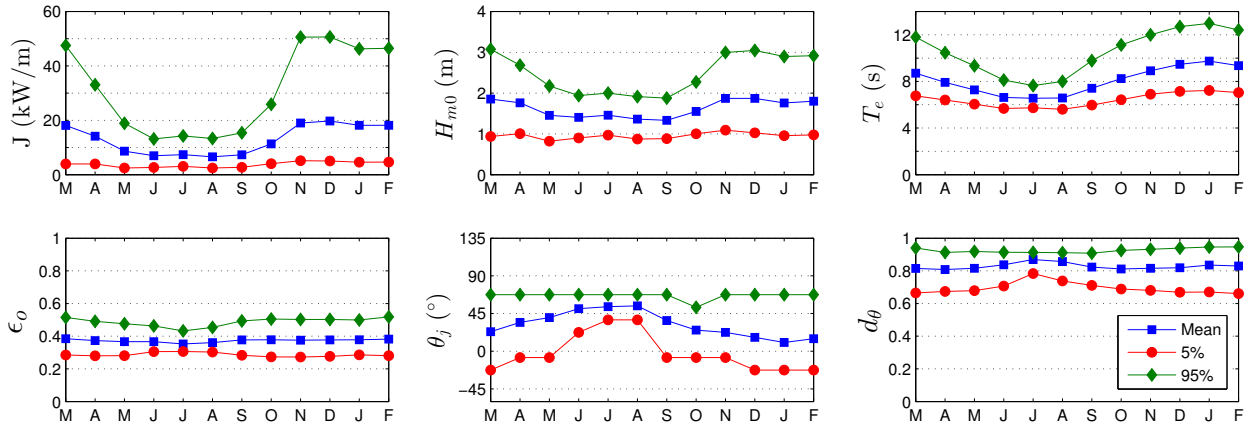


Figure 23: The average, 5th and 95th percentiles of the six parameters at Kaneohe II.

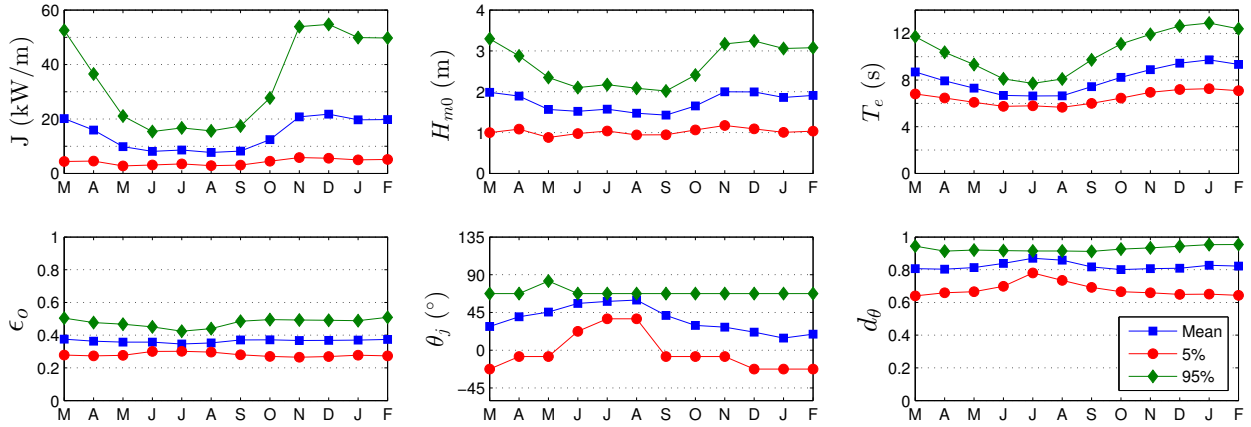


Figure 24: The average, 5th and 95th percentiles of the six parameters at WETS.

Monthly means, however, smear the significant variability of the six IEC parameters over small time intervals as shown in plots of the six IEC TS parameters at 1-hour intervals in Figure 25 for a representative year. While seasonal patterns described for Figures 23 and 24 are still evident, these plots show how sea states can vary abruptly at small time scales with sudden changes, e.g., jumps in the wave power as a result of a storm. Note that the data in Figure 25 is from NDBC 51207, co-located at the WETS 80 m berth.

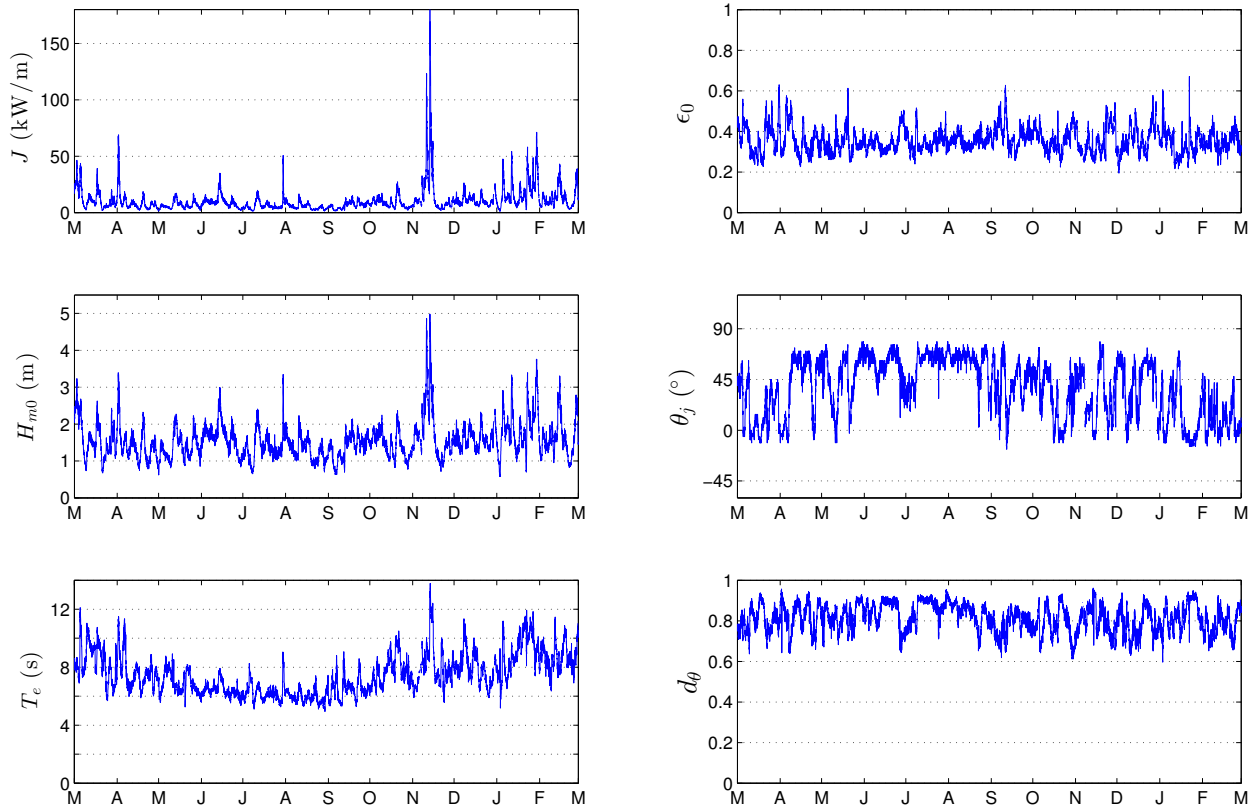


Figure 25: The six parameters of interest over a one-year period, March 2013 – February 2014 at NDBC 51207 co-located at the WETS 80 m berth.

4.4.3. Cumulative Distributions

Annual and seasonal cumulative distributions (a.k.a., cumulative frequency distributions) at WETS are shown in Figure 26. Note that spring is defined as March – May, summer is June – August, fall is September – November, and winter is December – February. The cumulative distributions are another way to visualize and describe the frequency of occurrence of individual parameters, such as H_{m0} and T_e . A developer could use cumulative distributions to estimate how often they can access the site to install or perform operations and maintenance based on their specific device, service vessels, and diving operation constraints. For example, if significant wave heights need to be less than or equal to 1 m for installation and recovery, according to Figure 26, this condition occurs about 5% of the time on average within a given year. If significant wave heights need to be less than or equal to 2 m for emergency maintenance, according to Figure 26, this condition occurs about 74% of the time on average within a given year. Cumulative distributions, however, do not account for the duration of a desirable sea state, or weather window, which is needed to plan deployment and servicing of a WEC device at a test site. This limitation is addressed with the construction of weather window plots in the next section.

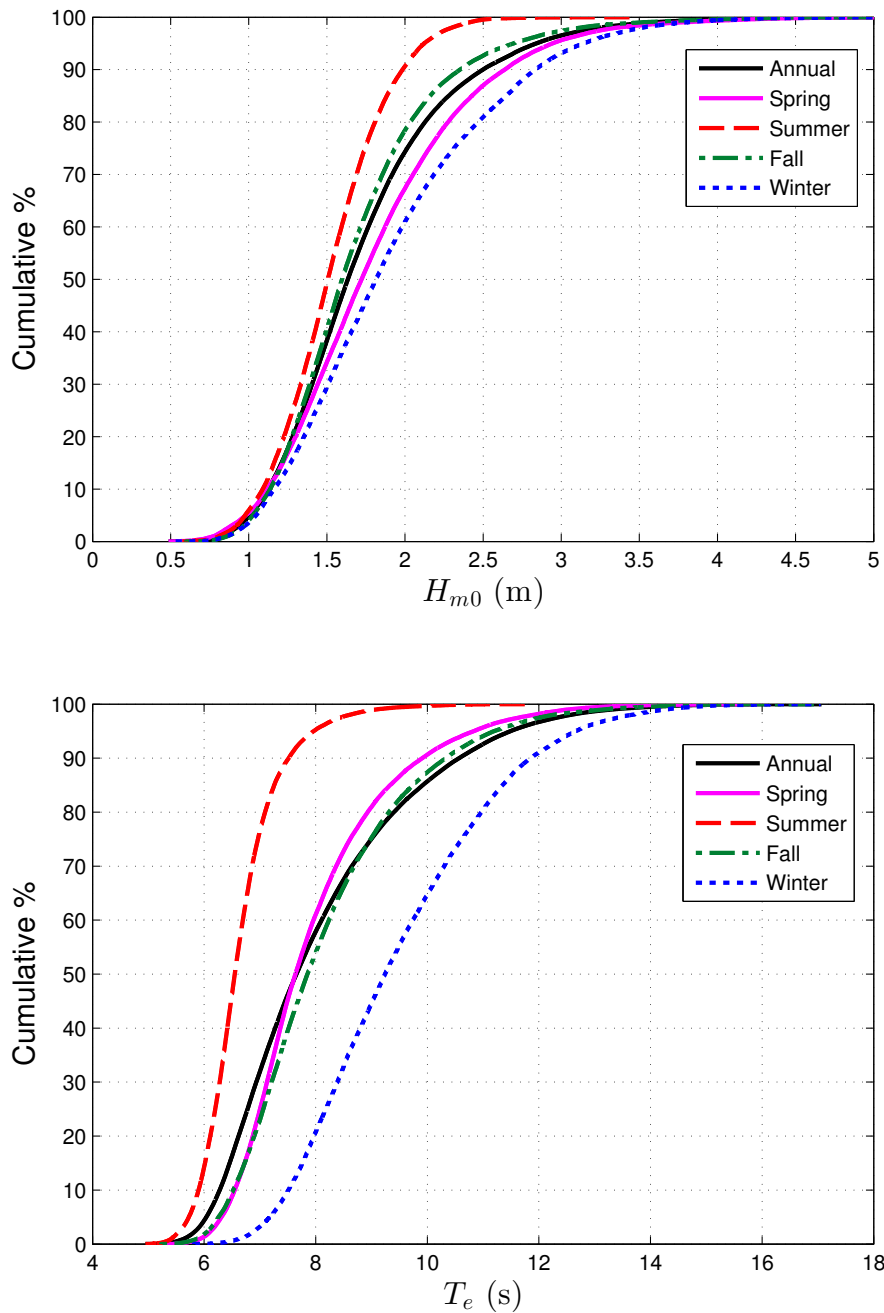


Figure 26: Annual and seasonal cumulative distributions of the significant wave height (top) and energy period (bottom) at WETS.

4.4.4. Weather Windows

Figure 27 shows the number of weather windows at WETS, when significant wave heights are at or below some threshold value for a given duration, for an averaged winter, spring, summer, and fall. In these plots, each occurrence lasts a duration that is some multiple of 6-hours. The minimum weather window is, therefore, 6-hours in duration, and the maximum

is 96-hours (4 days). The significant wave height threshold is the upper bound in each bin and indicates the maximum significant wave height experienced during the weather window. Note that the table is cumulative, so, for example, an occurrence of $H_{m0} \leq 1m$ for at least 42 consecutive hours in the fall is included in the count for 36 consecutive hours as well. In addition, one 12-hour window counts would count as two 6-hour windows. Although there are more occurrences of lower wave heights during the summer than winter (which corresponds to increased opportunities for deployment or operations and maintenance), the difference is not as significant at this site compared to others. The summer does have increased opportunities for deployment, however, it is still somewhat rare to find a longer weather window under 1 m. This is due to the consistent year-round trade winds. The timeseries in Figure 25 confirms that although wave heights remain fairly low in the summer (typically not exceeding 3 m), they rarely fall below 1 m. This also can be seen in Figure 24 where the 5th percentile of H_{m0} remains near 1 m throughout the year.

Weather window plots provide useful information at test sites when planning schedules for deploying and servicing WEC test devices. For example, if significant wave heights need to be less than or equal to 1 m for at least 12 consecutive hours to service a WEC test device at WETS with a given service vessel, there would be, on average, nine weather windows in the summer, but only five in the winter. When wind speed is also considered, Figure 28 shows the average number of weather windows with the additional restriction of wind speed, $U < 15$ mph. Note that wind data was available from this hindcast, and was used herein (Ning and Cheung 2014), see Section B.4. For shorter durations (6- and 12-hour windows), daylight is necessary. Windows with $U < 15$ mph and only during daylight hours are shown in Figure 29. Daylight was estimated as 5am - 10pm Local Standard Time (LST).

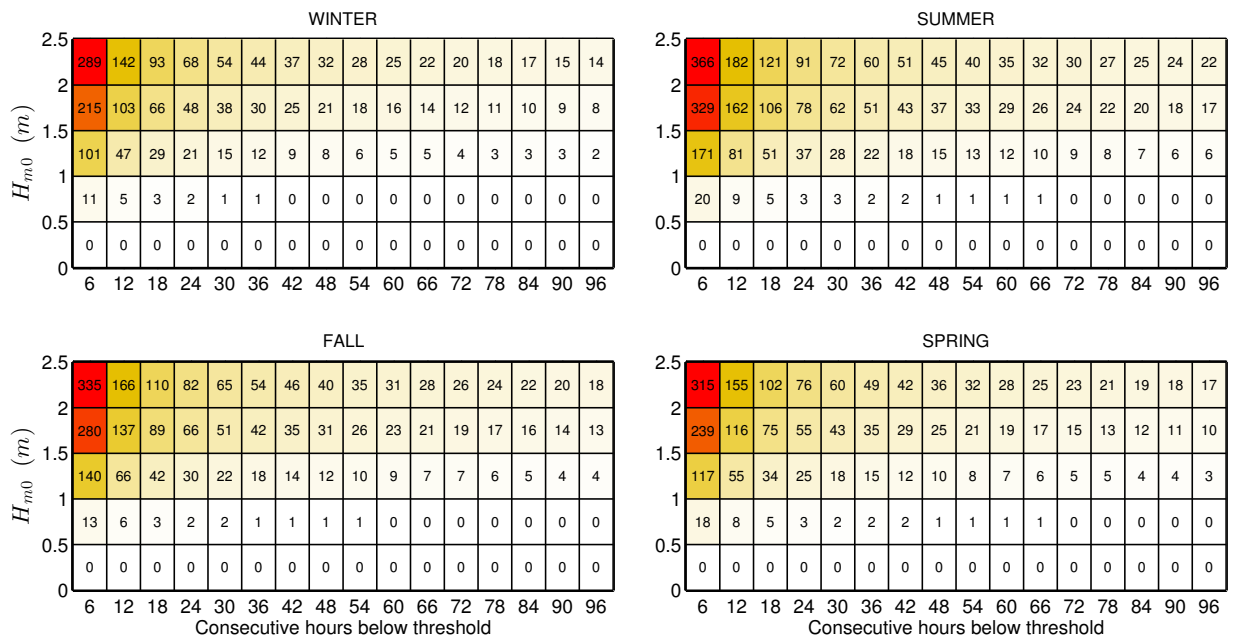


Figure 27: Average cumulative occurrences of wave height thresholds (weather windows) for each season at WETS. Winter is defined as December – February, spring as March – May, summer as June – August, and fall as September – November.

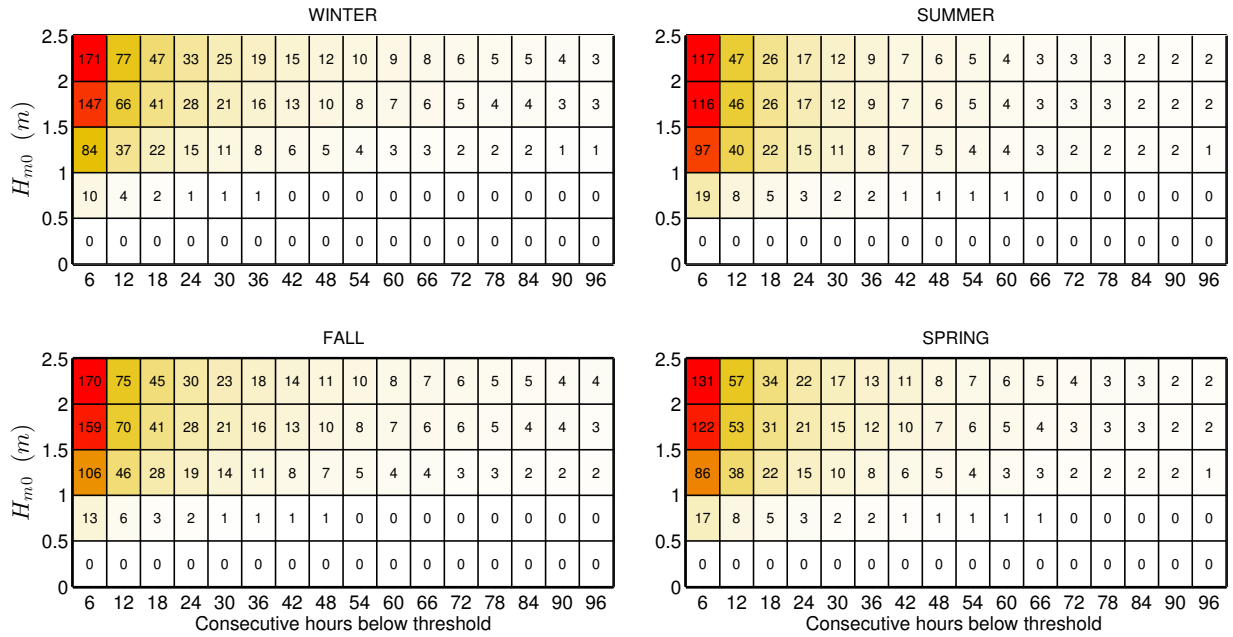


Figure 28: Average cumulative occurrences of wave height thresholds (weather windows) for each season at WETS with an additional restriction of $U < 15$ mph.

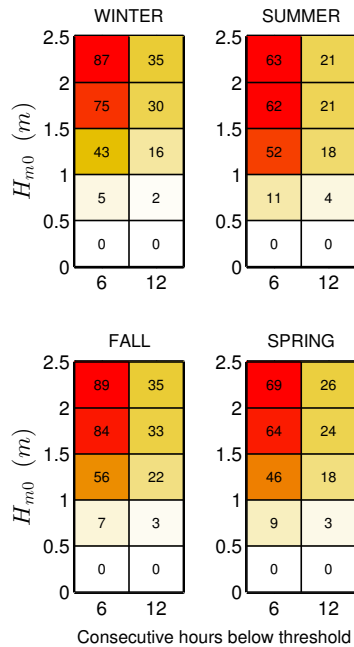


Figure 29: Average cumulative occurrences of wave height thresholds (weather windows) for 6- and 12-hour durations with $U < 15$ mph and only during daylight hours (5am - 10pm LST) at WETS.

4.4.5. Extreme Sea States

The modified IFORM was applied using CDIP098 / NDBC51202 to generate the 100-year environmental contour for WETS shown in Figure 30. Although there is a buoy co-located at WETS (CDIP198/NDBC51207), the period of record is only about three years, and therefore it was necessary to use a nearby buoy with a longer period of record (see Table 2 for buoy information). Selected sea states along this contour are listed in Appendix B, Table 15.

As stated in Section 1.2, environmental contours are used to determine extreme wave loads on marine structures and design these structures to survive extreme sea states of a given recurrence interval, typically 100-years. For WETS, the largest significant wave height estimated to occur every 100-years, is over 7.2 m, and has an energy period of about 13.0 s. However, significant wave heights lower than 7.2 m, with energy period less than or greater than 13 s, listed in Appendix B, Table 15, could also compromise the survival of the WEC test device under a failure mode scenario in which resonance occurred between the incident wave and WEC device, or its subsystem. For comparison, 50- and 25-year return period contours are also shown in Figure 30. The largest significant wave height on the 50-year contour is 6.9 m with an energy period of about 12.7 s, and on the 25-year contour is 6.6 m and 12.5 s. It should be noted that conditions at the NDBC51207 buoy may differ significantly from the conditions at the test site, even though they are at similar depths, NDBC51202 is outside of Kaneohe Bay.

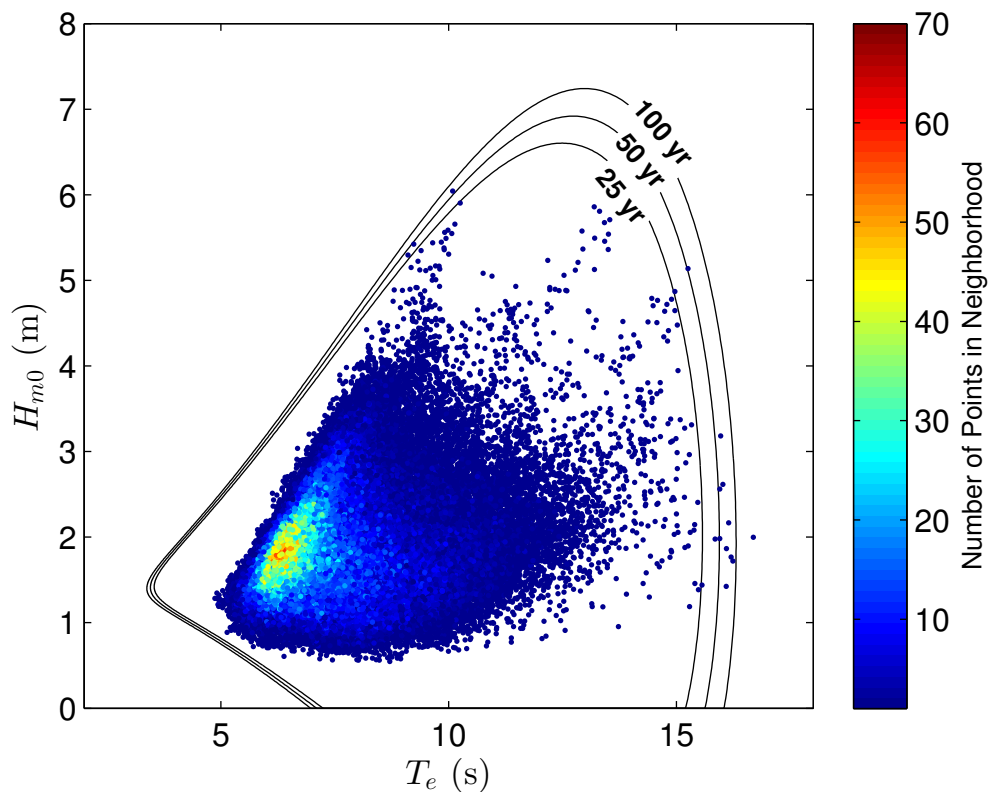


Figure 30: 100-year contour for CDIP098/NDBC51202 (2001 – 2014).

4.4.6. Representative Wave Spectrum

All hourly discrete spectra measured at CDIP198 / NDBC51207 for the most frequently occurring sea states are shown in Figure 31. The most frequently occurring sea state, which is within the range $1.5 \text{ m} < H_{m0} < 2 \text{ m}$ and $6 \text{ s} < T_e < 7 \text{ s}$, was selected from a JPD similar to Figure 22 in Section 4.4.1, but based on the CDIP198 / NDBC51207 buoy data. As a result, the JPD, and therefore the most common sea states, generated from buoy data are sometimes slightly different from that generated from hindcast data. However for this case, at WETS, the most frequently occurring sea state for the JPD generated from hindcast data is in the same range for both T_e ($6 \text{ s} < T_e < 7 \text{ s}$) and H_{m0} ($1.5 \text{ m} < H_{m0} < 2 \text{ m}$). Often several sea states will occur at a very similar frequency, and therefore plots of hourly discrete spectra for several other sea states are also provided for comparison. Each of these plots includes the mean spectrum and standard wave spectra, including Bretschneider and JONSWAP, with default constants as described in Section 2.2.

For the purpose of this study, the mean spectrum is the ‘representative’ spectrum for each sea state, and the mean spectrum at the most common sea state, shown in Figure 31 (top-right plot), is considered the ‘representative’ spectrum at the site. The hourly spectra vary considerably about this mean spectrum, but this is partly reflective of the bin size chosen for H_{m0} and T_e . Comparisons of the representative spectra in all plots with the Bretschneider and JONSWAP spectra illustrate why modeled spectra with default constants, e.g., the shape parameter $\gamma = 3.3$ for the JONSWAP spectrum, should be used with caution. Using the constants provided in Section 2.2, the Bretschneider spectra are fair representations of the mean spectra in Figure 31. The mean measured spectra is the best representation of the conditions, however, if these modeled spectra were to be used at this site, it is recommended that the constants undergo calibration against some mean spectrum, e.g., the representative spectrum constructed here.

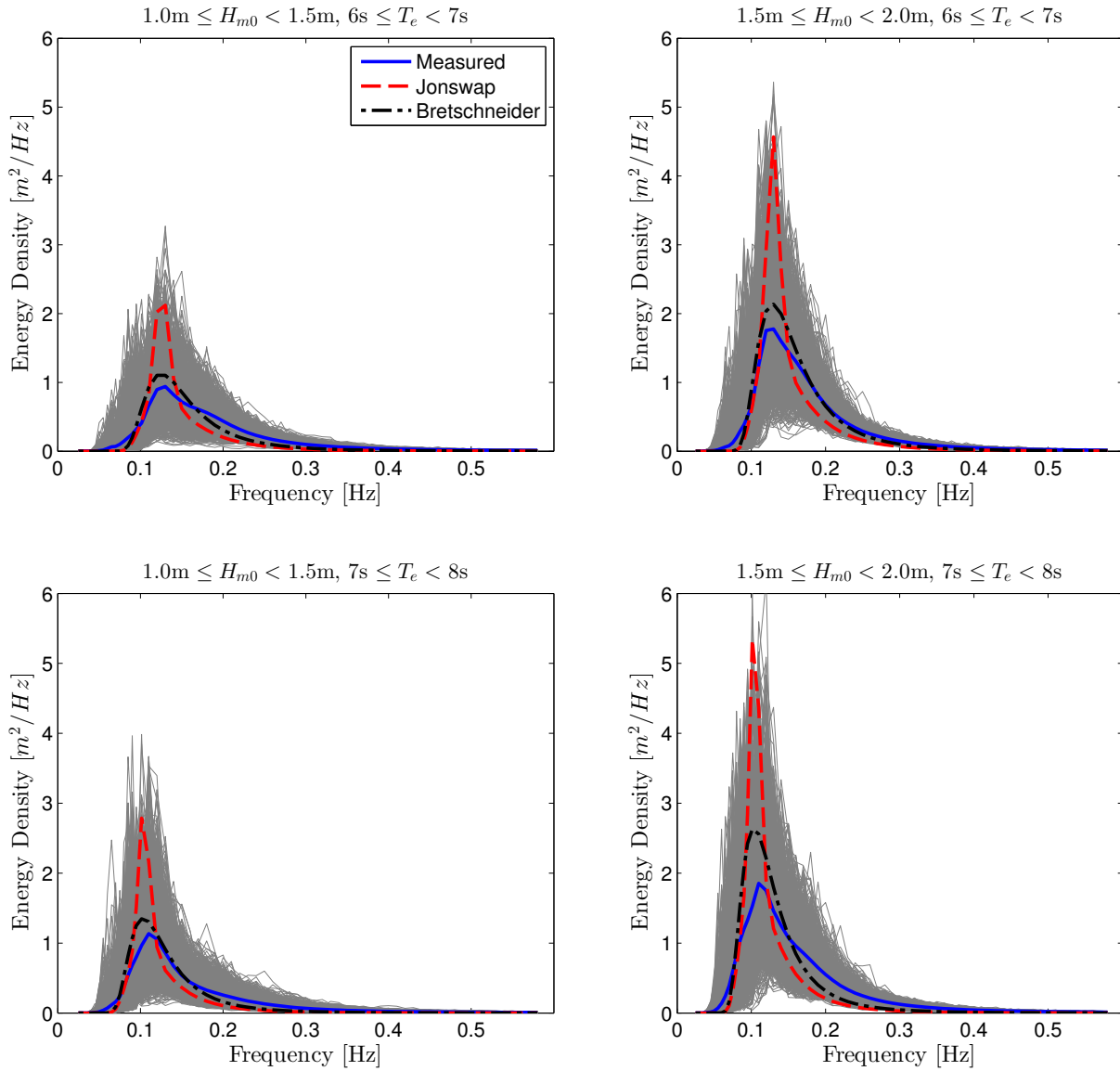


Figure 31: All hourly discrete spectra and the mean spectra measured at CDIP198 / NDBC 51207 within the sea state listed above each plot. The JONSWAP and Bretschneider spectra are represented by red and black dotted lines, respectively.